Biosensors and Bioelectronics 181 (2021) 113120

Contents lists available at ScienceDirect

Biosensors and Bioelectronics

journal homepage: http://www.elsevier.com/locate/bios

Structures and strategies for enhanced sensitivity of polydiacetylene(PDA) based biosensor platforms

Changheon Kim [a], Changgi Hong [b], Kangwon Lee [b,*]

[a] Program in Nanoscience and Technology, Graduate School of Convergence Science and Technology, Seoul National University, Seoul, 08826, Republic of Korea
[b] Department of Applied Bioengineering, Graduate School of Convergence Science and Technology, Seoul National University, Seoul, 08826, Republic of Korea

ARTICLE INFO

Keywords:
Polydiacetylene
Label-free sensor
Biosensor
Sensitivity
PDA structure
Transition mechanism

ABSTRACT

Polydiacetylene (PDA) is a versatile polymer that has been studied in numerous fields because of its unique optical properties derived from alternating multiple bonds in the polymer backbone. The conjugated structure in the polymer backbone enables PDA to possess the ability of blue-red colorimetric transition when π-π interactions in the PDA backbone chain are disturbed by the external environment. The chromatic property of PDA disturbed by external stimuli can also emit fluorescence in the red region. Owing to the unique characteristics of PDA, it has been widely studied in facile and label-free sensing applications based on colorimetric or fluorescence signals for several decades. Among the various PDA structures, membrane structures assembled by amphiphilic molecules are widely used as a versatile platform because facile modification of the synthetic membrane provides extensive applications, such as receptor-ligand interactions, resulting in potent biosensors. To use PDA as a sensory material, several methods have been studied to endow the specificity to PDA molecules and to amplify the signal from PDA supramolecules. This is because selective and sensitive detection of target materials is required at an appropriate level corresponding to each material for applicable sensor applications. This review focuses on factors that affect the sensitivity of PDA composites and several strategies to enhance the sensitivity of the PDA sensor to various structures. Owing to these strategies, the PDA sensor system has achieved a higher level of sensitivity and selectivity, enabling it to detect multiple target materials for a full field of application.

1. Introduction

Since qualitative and quantitative detection of specific substances or molecules is required in a wide range of fields, research on effective detection systems has been continuously developed over the past decades (Anker et al., 2008; Homola 2008; Vollmer and Arnold 2008). Among various target substances, detecting molecules derived from living organisms has great potential because not only can it be applied in the biological field but also in medical applications, such as for diagnosis of diseases (Aalipour et al., 2019; Im et al., 2014; Jacobs et al., 2010; Kim et al., 2020a). Attempts to detect molecules derived from living organisms are mostly based on molecular recognition, which is capable of specific binding of target molecules (Okada et al., 1998). Such molecular recognition appears between antibody-antigen, ligand-receptor, and enzyme-substrate in living organisms, which is a phenomenon that significantly influences the detection mechanism of the biosensor. That is, to detect and recognize biomolecules, the biosensor function is achieved by introducing a transducer that is capable of detecting the motif of biomolecules on the active substrate (Cui et al., 2001; El-Sayed et al., 2005; Wang et al., 2017b).

Among the numerous signal detection methods, biosensors based on color change or fluorescence signals have been widely used due to their sensitivity, multiplicity, versatility, and simplicity. Conjugated polymers, exhibiting colorimetric and fluorescence properties, are candidates that can be used in the aforementioned applications (Lee et al., 2016b; Qian and Stadler 2019; Sun et al., 2010). Since the first suggestion of solid-state synthesis methods for conjugated polymers based on monomers with diacetylene bonds (Wegner 1969), there has been considerable interest in developing conjugated polymers owing to their diverse applications such as sensing molecules or ions (Ho and Leclerc 2004; Ji et al., 2013; Rajesh et al., 2009; Yoon et al., 2011), conducting polymers in microdevices (Cheng et al., 2009; Ostroverkhova 2016), actuators (Jager et al., 2000; Liang et al., 2012; Smela 2003), and luminescence devices (Di Benedetto et al., 2008; Grimsdale et al., 2009).

Polydiacetylene (PDA), a type of conjugated polymer, has been widely investigated in the field of sensing applications because of its

* Corresponding author.
E-mail addresses: c.h.kim@snu.ac.kr (C. Kim), ckdrl0430@snu.ac.kr (C. Hong), kangwonlee@snu.ac.kr (K. Lee).

https://doi.org/10.1016/j.bios.2021.113120
Received 5 October 2020; Received in revised form 20 January 2021; Accepted 25 February 2021
Available online 2 March 2021
0956-5663/

unique optical features (Qian and Stadler 2019). Since the synthesis of PDA with double and triple alternating bonds was first presented by Wegner in 1969, PDA has received much attention for its unique optical properties. PDA can be prepared by the polymerization of amphiphilic diacetylene (DA) monomers and has distinct structures depending on the arrangement of the diacetylene monomers before polymerization.

The basic form of the diacetylene monomer is an amphiphilic structure with a hydrophobic group containing a diacetylene group and a polar head group at the end of the alkyl chain. Due to their amphiphilic properties, DA monomers can form arranged structures through a 'self-assembly effect' according to the surrounding environment. The structure of the PDA assembly can be modified in various structures such as crystals (Lauher et al., 2008; Park et al., 2014), tubes (Heo et al., 2017; Hu et al., 2014; Wang et al., 2018b), films (Ahn et al., 2003; Lu et al., 2001), Langmuir-Blodgett (LB) films (Chaki and Vijayamohanan 2002; Tachibana et al., 1999; Xu et al., 2013b), and vesicles (Kim et al., 2003b; Kolusheva et al., 2000a; Lee et al., 2008), depending on the molecular structure and fabrication method of the diacetylene monomer. Distinct PDA supramolecular structures can be applied in a suitable form to be utilized.

Closely arranged DA monomers can be polymerized by a 1,4-addition reaction under UV light in the wavelength range of 254 nm, forming an extensively delocalized π-π interaction alternating bond (Ahn and Kim 2008; Kolusheva et al., 2005). Intact polymerized diacetylene supramolecules usually absorb a relatively long wavelength band (~650 nm) by relaxing alternating bonds, resulting in an intense blue color. However, when an external stimulus is applied to the PDA, the absorption spectrum of PDA shifts to the short wavelength region (~550 nm), exhibiting a blue-to-red colorimetric change (Jelinek and Ritenberg 2013; Ma et al., 2006). Although the exact color transition mechanism of PDA has not been clarified, the strain from the alkyl chain of diacetylene is changed by the external environment, or a disturbance of the PDA backbone is the main cause of color change (Phonchai et al., 2019). That is, the stimulus generated by the external interaction is transferred from the side chain to the PDA conjugated backbone, causing deformation in the π-π bond. The deformation of the conjugated bond changes the topochemical properties and results in unique optical properties (Qian and Stadler 2019). Because PDA exhibits fluorescence and color change when the length of the alternating bond is disturbed by diverse factors, such as temperature (Ahn et al., 2003; Chance et al., 1977; Lee et al., 2014c; Wacharasindhu et al., 2010), pH (Charoenthai et al., 2011; Kew and Hall 2006), organic solvents (Dolai et al., 2017; Park et al., 2014; Wang et al., 2013; Yoon et al., 2009b), metal cations (Gwon et al., 2019; Jose and Konig 2010; Li et al., 2014), mechanical stress (Feng et al., 2013; Muller and Eckhardt 1978), electrical energy (Peng et al., 2009), or ligand-receptor interaction (Kolusheva et al., 2001; Lee et al., 2009a; Reichert et al., 1995; Reppy and Pindzola 2007b; Yoon et al., 2009a), the optical characteristics of PDA can be widely used as sensors in various fields.

In particular, the bi-signal system of PDA by the ligand-receptor interaction has the potential to be used as a biosensor or chemosensor to detect specific biomolecules including proteins (Jelinek and Kolusheva 2001; Jung et al., 2010), nucleic acids (Jung et al., 2008; Jung and Park 2015; Wang and Ma 2005), carbohydrates (Cheng and Stevens 1997; Cho and Ahn 2013b), chemical compounds (Lee et al., 2014a; Xu et al., 2013a), and bacteria (Jung et al., 2014; Ma et al., 1998; Park et al., 2012; Rangin and Basu 2004; Wu et al., 2011b) because of their simplicity and accessibility. Additionally, diacetylene, which acts as the main PDA skeleton, can be widely customized by introducing specific molecular groups according to the required purpose or scope of application (Qian and Stadler 2019). Polymerization of PDA is possible with 254 nm UV without any additional additives, which does not interfere with the detection of biomolecules that are sensitive to chemical composition. Unlike conventional methods for biomolecular detection such as the Blotting technique and the enzyme-linked immunosorbent assay (ELISA) (Lee et al., 2016b), PDA-based sensor platforms do not require additional labeling processes using fluorescence probes because PDA can emit fluorescence by themselves when its state changes.

Despite the advantages of these PDA, relatively low sensitivity has been an obstacle to using PDA as a sensory material (Olmsted and Strand 1983). Like other organic fluorophores, PDA supramolecules do not have sufficient fluorescence conversion efficiency as compared to conventional inorganic compounds, such as quantum dots. Additionally, sufficient physical stimulation is required for the distortion of the conjugated backbone of PDA to convert PDA into fluorescence (Olmsted and Strand 1983). Accordingly, to improve the suitability of the PDA sensors, several methods to increase the selectivity and sensitivity of PDA have been studied (Table S1). This review will cover the topological structure of PDA and the development of sensing platforms using the basic structure and characteristics of PDA. Moreover, this review discusses factors that affect the optical properties of PDA and recent research on strategies for the sensitivity of biosensors in various PDA assemblies.

2. Properties of PDA

2.1. Diacetylene structure and polymerization

The diacetylene monomer refers to molecules containing a diacetylene group (diyne), and the dialkyne group is generally produced by a Cadiot-Chodkiewicz coupling reaction (Alami and Ferri 1996). The pairing reaction between an alkyne terminal and a halo-alkyne terminal is catalyzed by a copper salt and amine base, generating 1,3-diyne or dialkyne (Bandyopadhyay et al., 2006). Various diacetylene monomers can be formed according to the alkyl chains of alkyne and haloalkyne compounds. Since the alkyl chains in the reactants do not participate in the coupling reaction, diacetylene products have various physical properties depending on the structure of the alkyl side chain (Nishihara et al., 1998). PDA are formed through the 1,4-photopolymerization of arranged diacetylene monomers under UV (245 nm) or γ-ray irradiation,

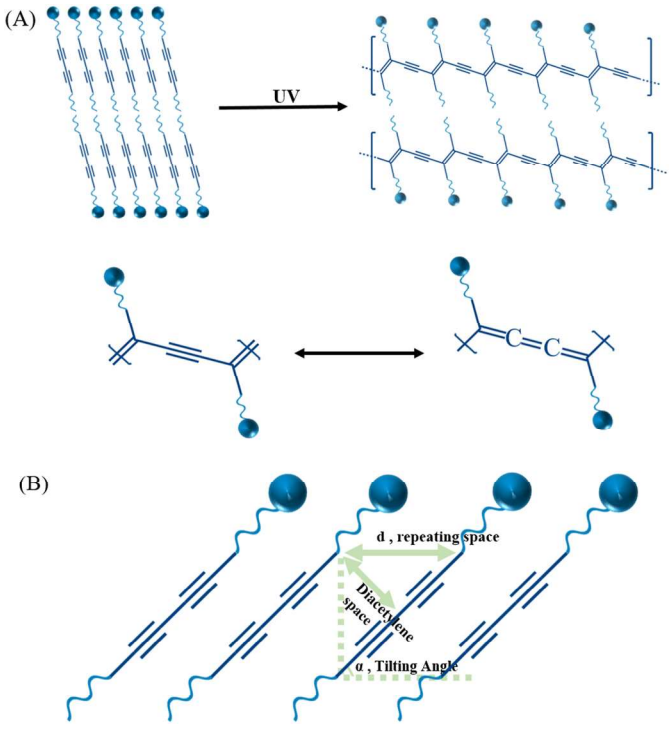

Fig. 1. Structure of polydiacetylene; A) topochemical and resonance structure of polydiacetylene, B) Topochemical polymerization in the self-assembly structure of diacetylene and Factors affecting the mode of polymerization in aligned diacetylene assembles; repeat distance, diacetylene intermolecular distance, tilting angle of diacetylene group.

and diyne groups generate a conjugated bond of the main chain (Fig. 1a) (Blaise et al., 1991; Carpick et al., 2004). Since the diacetylene polymerization process occurs *in situ*, the propagation stage of polymerization effectively proceeds when it satisfies the geometrical arrangement and the distance between adjacent monomers (Kim et al., 2005a; Sheth and Leckband 1997). That is, for PDA to be formed efficiently, a solid-state in a crystalline form or an adequately arranged structure is required. Generally, the PDA backbone is described as having conjugated bonds with alternating ene-yne, but it possesses resonance structures of the acetylenic and butatrienic groups (Reppy and Pindzola 2007b). However, due to the short bond length of the butatrienic group, the butatrienic group is more unstable than the acetylenic group (Kuriyama et al., 1996a). For this reason, butatrienic groups rarely occur in densely packed blue state structures (Dobrosavljevic and Stratt 1987; Eckhardt et al., 1986; Kuriyama et al., 1998).

A considerable number of DA monomers have amphiphilic properties that have both a hydrophilic polar head group and a hydrophobic nonpolar tail. Diacetylene monomers can be divided mainly into a head group, a diacetylene group, and side alkyl chains, including the tail and spacer (Menzel et al. 1999, 2000; Shimogaki and Matsumoto 2011). Depending on the structure of the head group and tail, not only the physical properties of diacetylene and PDA, but also the polymerization efficiency and versatility vary and these properties can be customized according to the intended use. Diacetylene structures can be roughly divided into three types depending on the position of the polar group and diacetylene group, namely, linear (Chae et al., 2016; Jang et al., 2019; Lee et al. 2014a, 2014c), phospholipid-like (Kuo and Obrien 1990; Pakhomov et al., 2003a; Rhodes et al., 1992; Wang and Hollingsworth 1999), and non-linear types (Heo et al. 2017, 2019; Kantha et al., 2018; Singh and Jayaraman 2016; Xu et al., 2014a) (Fig. 2).

The linear type refers to a monomer in which a polar head group is attached in a straight line the monomer end or center. Linear diacetylenes are the most widely used diacetylene types owing to their simple molecular structure and versatility for forming various structures such as films and vesicles. The phospholipid type has a diacetylene group on two tails with a structure similar to phospholipids (Yager et al., 1985). This type was first proposed while designing a membrane that is capable of polymerization to increase the stability and strength of the layer composed of naturally derived lipids. Finally, the nonlinear type of diacetylene has multiple arms or a circular structure. Because of its unique architecture, this type of diacetylene usually forms one-dimensional (1D) tubes or helix structures rather than two-dimensional (2D) membranes (Heo et al., 2019; Xu et al., 2014a). Notably, to use PDA as a sensor, receptors that can specifically recognize specific targets need to be introduced into the terminal head groups of the diacetylene monomers (Ardona and Tovar 2015). For example, many of the commercially available basic diacetylene monomers have a carboxylic acid at the terminal site due to the high reactivity and versatility of the acid group. By modification of the polar group, more diverse and tailored diacetylene structures can be prepared to introduce diverse receptors or molecular groups (Qian and Stadler 2019). For example, through the EDC/NHS coupling reaction, an additional alkyl chain can be attached by the combination of the amine and carboxylic groups at the diacetylene terminal. In addition, the newly formed amide bond can create an intermolecular hydrogen bond, thereby enhancing the self-assembly effect (Jung et al., 2008; Park et al., 2016c). Additionally, various receptors introduced into PDA have many amine groups, which is advantageous for bioconjugation between PDA and biomolecules.

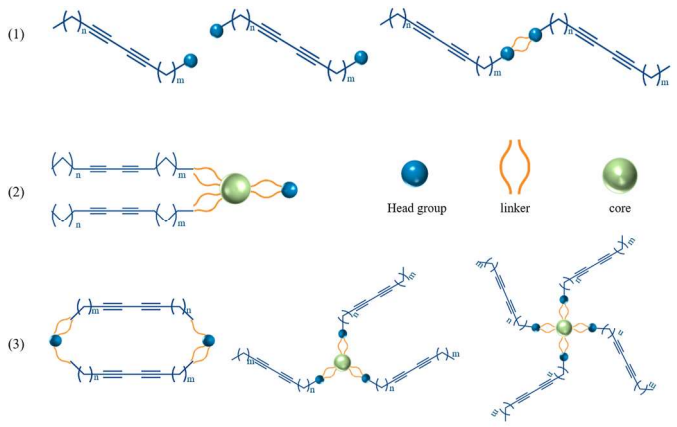

Fig. 2. Three classes of Diacetylene monomer structure; 1) Linear diacetylene having a straight structure in which the head group, alkyl chain, and linker are connected in a line, 2) A phospholipid-like diacetylene monomer containing two diacetylene groups in each alkyl chain of phospholipid and a polar head group, 3) Non-linear diacetylene monomer with circular structure (left) and multiple arms (right). This figure is reproduced with permission from ref. (Qian and Stadler 2019). Copyright 2019, American Chemical Society.

When properly self-assembled diacetylene monomers are polymerized by UV light to form a conjugated bond, physical stability, mechanical strength, and thermal stability increase (Sheth and Leckband 1997). Because of the nature of conjugated bonds that absorb specific wavelengths, PDA are usually blue in color, but in some cases, purple, pink, red, yellow, and black colors can appear (Okada et al., 1998). Self-assembled diacetylene monomers with low stability require substantial of UV exposure for sufficient color development, but excessive UV exposure usually shifts the absorption spectrum of the conjugated bond in a short wavelength, causing a color change from purple to red due to depolymerization and chain cutting (Bloor and Worboys 1998; Morgan et al., 1992). The signal of a typical PDA sensor can be characterized by the UV–vis absorption spectrum or fluorescence intensity. Additionally, the ene-eyn structure of the conjugated bond can be further characterized through Raman spectroscopy (Batchelder and Bloor 1982; Batchelder et al., 1981; Sandman and Chen 1989), ^{13}C NMR (Lee et al., 2002; Nava et al., 1990; Tanaka et al., 1989), and X-ray studies (Fischetti et al., 1988; Lieser et al., 1980).

2.2. Optical properties of PDA

The unique optical properties of PDA are mainly derived from the conjugated backbone (McQuade et al., 2000). When the resulting conjugated bond is disturbed by external stimuli, the optical properties of the PDA can manifest themselves significantly (Yoon et al., 2013). In the early years, PDA sensors focused on changing the optical properties of the PDA itself, but methods of increasing sensitivity or selectivity to the target materials of PDA-based sensors have also received much attention in the past decade (Yarimaga et al., 2012a). Several approaches to detect the signal from the optical properties of PDA exist, namely, colorimetric change, fluorescence, and Raman spectroscopic analysis are mainly used to analyze the state of the PDA (Yoon et al., 2009a) (Fig. 3) (Fig. 4).

Understanding the PDA optical change mechanism is essential for realizing PDA-based sensor designs with more sensitive and stable sensing abilities, which can develop PDA into a competent material that can be applied to more diverse applications and environments. Although many studies have been conducted to uncover the mechanism of the unique optical properties of PDA, the exact mechanism has not been fully understood and has been controversial (Chae et al., 2016). The main reason for this imprecision is that it is difficult to observe the PDA while all conditions are controlled because there are many factors that can affect the optical characteristics of the PDA (Reppy and Pindzola 2007b). Presently, the disturbed state of the conjugated bonds caused by structural changes in the PDA is considered to be the most commonly accepted cause of the unique optical features.

2.2.1. Colorimetric change

Among the various detection methods, the color change caused by the shift in the absorption spectrum is an intuitive detection method that

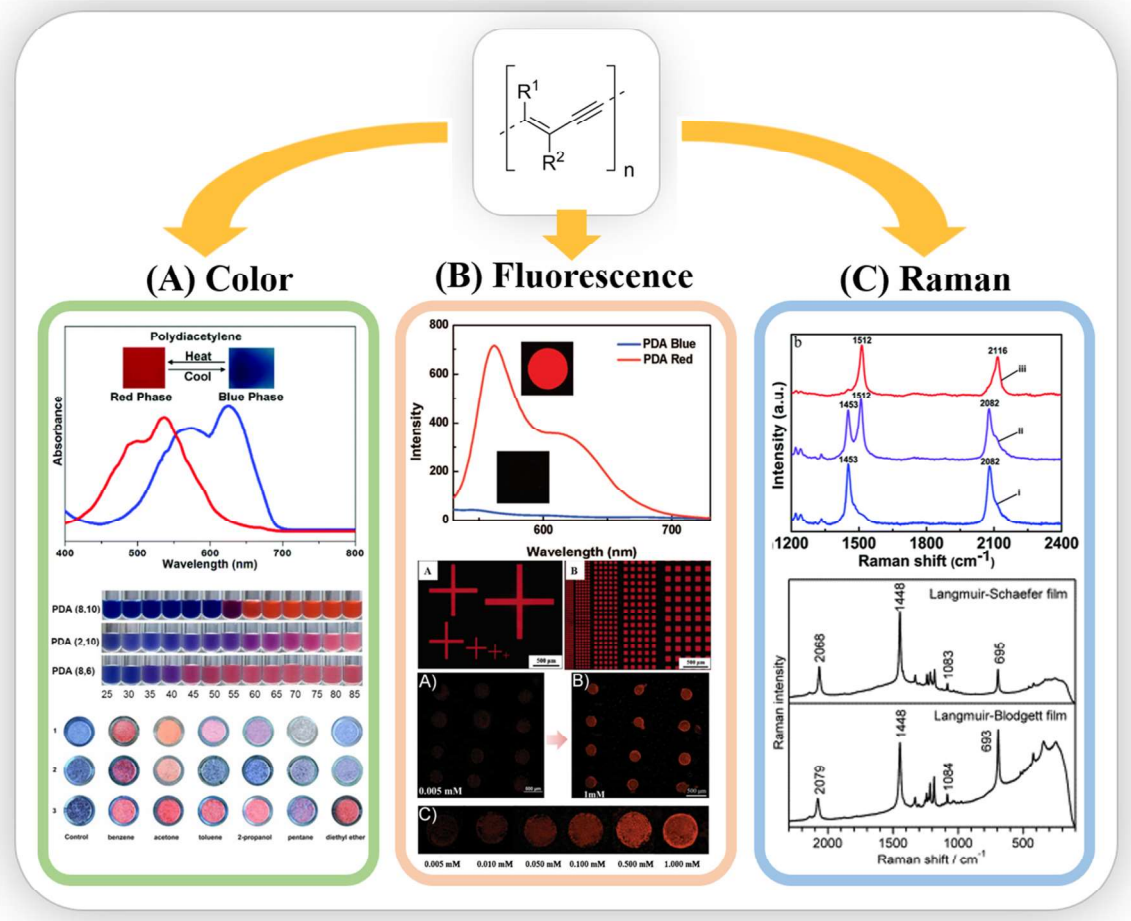

Fig. 3. Optical properties of PDA (CR, FL, Raman) Section A reproduced with permission from ref. (Huo et al., 2017a). Copyright 2017, The Royal Society of Chemistry, reproduced with permission from ref. (Dolai et al., 2017). Copyright 2016, American Chemical Society and reprinted reproduced with permission from ref. (Khanantong et al., 2018). Copyright 2018, Elsevier B.V. Section B reproduced with permission from ref. (Ahn and Kim 2008). Copyright 2008, American Chemical Society, reproduced with permission from ref. (Kim et al., 2005b). Copyright 2005, American Chemical Society and reproduced with permission from ref. (Lee et al., 2009b). Copyright 2009, WILEY-VCH Verlag GmbH & Co. KGaA, Weinheim. Section C reproduced with permission from ref. (Seto et al., 2007). Copyright 2007, Elsevier B.V. and reproduced with permission from ref. (Xu et al., 2018). Copyright 2018, The Royal Society of Chemistry.

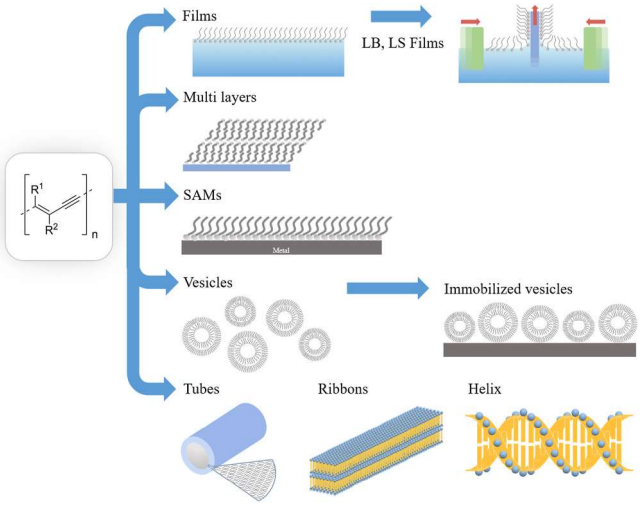

Fig. 4. Classification of various PDA structures used in biosensor applications.

can be sufficiently observed with the naked eye (Zhang et al., 2014). PDA is also one of the materials that can change color, and during the polymerization reaction, PDA strongly absorbs a specific wavelength when a backbone conjugated bond is formed, resulting in a remarkable color change. That is, the PDA color derived from the conjugated bond means that the PDA color may change depending on the state and characteristics of the conjugated bond (Huo et al., 2017a). PDA shows a change in the absorption spectrum upon external stimulation which is large enough to be observed with the naked eye, indicating that the PDA can be used as a naked eye detectable sensor platform as shown in Fig. 3a. The absorption spectrum of PDA changes in three specific wavelength ranges depending on the state, and the corresponding peak may vary depending on factors such as the type of diacetylene, assembly structure, polymerization progress, and external stimulus. PDA in the intact blue and disturbed red state peak at approximately 650 nm and 550 nm, respectively, and may form minor peaks in the region tens of nm lower than that (Chen et al., 2012b) (Fig. 3a, upper). When the spectrum of PDA changes, the peak in the longer wavelength region gradually decreases around the point where the absorbance does not change (isosbestic point). At the same time, the peak in the short wavelength region is newly formed, and the peak gradually increases (Chanakul et al., 2013; Shin and Kim 2016; Zhang et al., 2018a). Through the following transition, the blue PDA changes color in the order of purple, pink, and red (Dautel et al., 2006; Heo et al., 2017; Lee et al., 2014c). PDA with unusual colors such as yellow (Chu and Xu 1991; Oikawa et al., 1999; Wang et al., 2017a) or green (Gregory J. Exarhos et al., 1976) show different peaks or patterns in the general absorption spectrum.

Since the absorption spectrum of PDA varies depending on the type of monomer or assembly, the color change should be quantified to use PDA as a colorimetric sensor. The colorimetric change of PDA can be quantified according to the peak of the absorbed wavelength in each state.

$$CR\ (\%) = \frac{(PB_{bef} - PB_{aft})}{PB_{bef}} \times 100, \quad PB = \frac{A_{blue}}{A_{blue} + A_{red}}$$

Here, A_{blue} and A_{red} represent the absorbance of the peak values in the UV–vis spectrum in the blue and red states, respectively, and PB represents the values before and after the reaction occurs (Charych et al., 1993; Okada et al., 1998).

If a colorimetric response (CR) technique based on a UV–vis spectrometer is challenging to apply, alternative chromatic analysis on a photograph can be used (Dolai et al., 2017). This method is mainly used when measuring an opaque substrate and is obtained by using the relative intensity of the red, green, and blue channels by extracting the color on the surface as a digital image.

$$\text{RCS}\ \ (\%) = \frac{(CL_{sample} - CL_0)}{(CL_{max} - CL_0)} \times 100, \quad CL = \frac{R}{(R+G+B)}$$

Here, R, G, and B indicate the intensity of each channel (red, green, and blue), and the degree to which the red channel occupies the intensity of the entire channel indicates the red chromaticity level (CL). The final RGB can be calculated using the PDA sample of interest and the chromaticity of the red PDA (Volinsky et al., 2007; Weston et al., 2020).

The final RGB can be quantified through the process of digitizing or normalizing the PDA color change using various analysis technologies, and the sensor can be use as a signal intensity based on the quantified PDA signal value.

2.2.2. Fluorescence

Fluorescence of PDA appears simultaneously with the colorimetric change derived from disturbed conjugated bonds. For example, the intensity of fluorescence emitted by the blue state PDA is insignificantly weak, but it is much more robust in a red or yellow state PDA (Chen et al., 2012b). As the color change degree increases, the fluorescence intensity increases proportional to the degree of the PDA deformation, while the blue PDA gradually turns purple, pink, and red by external stimuli (Kootery et al., 2014; Wei et al., 2015; Zhang et al., 2018a). The modified PDA membrane structure is excited by light in the region above 450 nm, and fluorescence appears as two broad peaks in the red region above 500 nm. Similar to the UV–vis spectrum change of PDA, the fluorescence spectrum varies depending on the degree of polymerization of PDA and the structure of the diacetylene monomer. Although the fluorescence "turn on" characteristic of PDA may serve as an advantage, the fluorescence intensity of PDA is relatively inefficient as compared to other fluorophores. The blue PDA backbone, which has a relatively stable conjugated bond, exhibits a quantum efficiency of 10^{-5} or less due to rapid excitation relaxation (Hattori and Kobayashi 1987; Kobayashi et al., 1997; Yasuda et al., 1993). In contrast, the quantum efficiency of PDA in the red state is expected to be approximately 0.02 at room temperature, which is significantly higher than that of PDA in the blue state, but still shows a low efficiency value (Olmsted and Strand 1983). This is because the film structure of the excited state PDA, which is closely aligned with the properties of the conjugated bond, is partially quenched by inter-chain energy transfer. Increased non-radiative decay pathways, such as thermal fluctuation of the side chains, are the main reason for the increase in an environment within an ordinary temperature range compared to a relatively high quantum yield in an extremely low-temperature condition (Carpick et al., 2000).

To compensate for the low quantum efficiency of PDA, fluorophore molecules can be introduced to increase the overall fluorescence efficiency. By introducing fluorophores to PDA, PDA can act as a donor to transfer energy to a fluorophore or as an acceptor to receive energy from a fluorophore (Wang et al. 2016, 2018a). Brcause the quantum efficiency of the conjugated bond in PDA is usually lower than that of conventional fluorophores, a fluorescence intensity enhancement is exhibited when a fluorophore acting as an acceptor is introduced to receive energy from the PDA. In contrast, when the fluorophore acts as a donor rather than as an energy acceptor, PDA excitation is possible in a region shorter than the PDA excitation wavelength. When a fluorophore molecule is used with PDA, it is necessary to adjust the distance appropriately because the excited state of the PDA-conjugated bond is relaxed by inter-chain energy transfer so that fluorescence can be quenched according to the distance between them (Ma et al., 2006). That is, the conjugated bond of PDA can be used as a fluorophore energy quencher (Ma and Cheng 2005; Ma et al., 2006).

2.2.3. Raman spectroscopy

Raman spectroscopy is an attractive method for PDA analysis because it enables direct visualization of detailed molecular structure information and the qualitative relationship between signal strength and substance concentration (Lichtman and Conchello 2005). Along with the development of optical microscopy, various strategies and techniques for capturing the faint signal of probes or molecules have emerged and have been applied in various fields for several decades. Resonant Raman spectroscopy has been used to identify these characteristics through the frequency and intensity of conjugated bonds present in the PDA backbone. In the early spectral studies of PDA, studies were conducted on two resonance structures of the PDA backbone and it was confirmed that the red form of PDA does not have a butatriene structure (Gregory J. Exarhos et al., 1976). Through Raman analysis, information about the double and triple bonds of the PDA backbone can be obtained. Additionally, the degree of polymerization and whether PDA transition occurs can be confirmed (Chen et al. 1984, 1985; Exarhos et al., 1976).

That is, the length of the π-electric delocalization of the PDA backbone in a state deformed by the external environment affects the electronically excited state so that the π-electric delocalization state by polymerization can be estimated. For example, the [= C(R)—C≡C—(R) C =]$_n$ structure produced by polymerization between diacetylene monomers forms a pseudo-1D electronic system due to substantial π-electric delocalization. Therefore, ν (C═C) and c (C≡C) vibrational bands can be observed as sharp peaks and the frequency or intensity of the bands corresponding to the above dramatic changes as well as the presence or absence of PDA deformation (Huo et al., 2017b; Itoh et al., 2005; Jordan et al., 2016). For example, the stretching modes of the C≡C, C═C, and C–C Raman spectra of the blue PDA Langmuir-Schaefer (LS) film composed of 10,12-pentacosadiyonic acid (PCDA) were 2068, 1448, and 1083 cm^{-1}, respectively. In contrast, LB films composed of the same monomers were found to be 2079, 1448, and 1084 cm^{-1}, respectively, meaning that even films with the same composition can have different properties depending on the assembled structure. That is, the difference in packing density of the diacetylene monomers changes the length of the C≡C bond and the wavenumber of this bond is noticeably different. The Raman shift in the region from 1180 to 1330 cm^{-1} reveals the geometrical alignment of the CH_2 alkyl chain in the C–C bond (Seto et al., 2007). When the PDA starts to change state, new peaks are formed in a section slightly smaller than the peak wavenumber of each C≡C and C═C bond. As the disturbed state of PDA progresses, the signal of the current peak decreases, and the size of the newly formed peak increases and becomes gradually dominant. It is possible to indirectly predict the state change of the PDA by using the ratio of the two peaks (Bang et al., 2016; Lifshitz et al., 2011; Xu et al., 2018). Due to the rich alkyne binding in PDA backbone, it is recognized as a potential Raman probe. In particular, alkyne Raman signal has a distinct cellular Raman-silent region (1800-2800 cm^{-1}), so it is receiving a lot of interest as a bioorthogonal Raman imaging agent. In particular, PDA supramolecules in various forms can be formed through customizable diacetylene monomers, and can be prepared in a form dispersed in an

aqueous solution. In addition, by introducing a specific receptor, it is possible to act as a sensor with selectivity. In order to increase the function as a Raman probe, it is necessary to amplify the PDA Raman signal, and a study has been made to make PDA-based composites that incorporate Surface-enhanced Raman scattering (SERS). The narrow emission peak emitted by SERS composite not only enhances material sensing capability, but also has the potential for multiple detection.

Because of the pseudo-1D π-electric delocalization generated by the conjugated bonds, PDA crystals have been used for many of the conjugated networks since the first reports of the dramatic enhancement of large third-order optical nonlinearity. Owing to the resonance of the conjugated bond, strong ν (C═C) and c (C≡C) vibrational bands are observed in the low frequency Raman spectrum and the linear correlation is the resonance mixture of the butatriene structure. Because of these nonlinear properties, PDA has become candidates for use in next-generation optoelectronics and molecular electronics.

2.3. Categories of polydiacetylene assemble

Like other amphiphilic molecules, DA monomers can form various structures in diacetylene assemblies by self-assembly (Gros et al., 1981; Ringsdorf et al., 1988). Diacetylene molecules can be solidified through crystallization by cooling after various forms are formed by self-assembly at high temperature with fluidity. Diacetylene assemblies can be generally divided into single- or multi-layered film forms, spherical vesicle forms, and other colloidal structures (Fig. 5) (Reppy and Pindzola 2007a).

2.3.1. Films and self-assembly layers (SAMs)

After the first synthesis of the diacetylene monomer, the physical and optical properties of PDA in the form of bulky crystals were reported (Chance and Baughman 1976; Hood et al., 1978; Lochner et al., 1976; Muller and Eckhardt 1978). Since then, the PDA film is the first structure of membrane assemblies, not a bulky crystal form, and several types of films have been prepared as numerous diacetylene monomers (Chance et al., 1979; Kajzar et al., 1983; Olmsted and Strand 1983). The membrane structure of PDA is a basic method to study various characteristics of PDA through several techniques, such as spectroscopic and microscopic analysis, and film structures (Germinario and Gillette 1982). The film structure of PDA can be classified into three types, namely LB films (Gaboriaud et al., 2001; Geiger et al., 2002; Germinario and Gillette 1982; Lifshitz et al., 2009; Wang et al., 1999), LS films (Ahn et al., 2003; Berman et al., 1995; Lee et al., 2018a) and SAMs (Batchelder et al., 1994; Khanantong et al., 2020; Kim et al., 1995; Lee et al., 2018b; Mowery et al., 1998), depending on the physical and chemical characteristics of the DA monomers and external environments.

Amphiphilic DA monomers dispersed in a solution can be arranged between the liquid and air boundary. When a compression force is applied to the gaseous or liquid phase membrane, an evenly distributed and densely aligned film is formed. The floating diacetylene film can be transferred to other substrates, and polymerized diacetylene films have been studied for the material properties of PDA and have been applied to the sensor applications (Chen et al., 2011; Kootery et al., 2014; Lieser et al., 1980; Zhang et al., 2016b). Due to the unique characteristics of PDA films and customizable monomers, interest in PDA films began to increase, and accordingly, research on the stability of PDA films was conducted. Since films composed of DA monomers have similar structures and properties to the cell membrane, methods and approaches based on biomimetics were introduced to the PDA platforms (Kang et al., 2012a; Lee et al., 2016a; Okaniwa et al., 2015). For example, a film composed mainly of DA monomers with distinct alkyl tail and head groups can be prepared, and substances such as phospholipids and cholesterol contained in the actual cell membrane can be added (Ferguson et al., 2005). By introducing specific receptors on the film surface, bio-inspired PDA membranes that can induce various interactions on the film surface are produced (Charych et al., 1996; Pan and Charych 1997; Spevak et al., 1995).

Another method to prepare a 2D films of PDA assemblies is to use SAMs (Menzel et al. 1998, 2000; Sullivan et al., 2005). The formation of spontaneous molecular assemblies is possible by using interactions between specific substances and functional groups, typically metal surfaces and thiol groups (Menzel et al., 1998). When a diacetylene monomer with a thiol head group is exposed to an environment where a metal surface is present, DA monomers are spontaneously adsorbed onto the metal surface to form a single layer film that is more stable than conventional LB or LS films. PDA films using SAMs have not been studied as much as LB or LS films but have great potential in sensing applications through synergy with metallic materials for surface plasmon resonance sensor platforms.

PDA composed of LB or LS films is relatively easy to produce but owing to the properties of a film with only a couple of layers, the signal strength of the PDA is inevitably low, which is a disadvantage in that additional equipment is required for signal measurement (Pindzola et al., 2006). To solve the problem of the monolayer structure, a method of constructing multilayers by laminating several layers of diacetylene films was introduced. The easiest and most widely used method is to evaporate the diacetylene mixture in the form of an organic solvent or aqueous solution to obtain the remaining molecules in the form of a thick layer in which multiple layers exist through self-assembly. The multi-layer coating can replace the Langmuir or SAM technique and it is also used to make vesicle types of PDA.

2.3.2. Vesicles (liposome)

The cell membrane is mainly composed of amphiphilic phospholipids, forming a double layer through hydrophilic and hydrophobic effects in an aqueous solution. Silimilary, DA monomers acting as lipid molecules in the cell membrane can also form a three-dimensional (3D) spherical vesicle (Bangham 1989). PDA vesicles can usually be prepared by hydration of lipid membranes under sonication in an aqueous solution environment (Cho et al., 2016b; Park et al., 2016d). When the organic solvent in which the diacetylene monomer is dissolved is evaporated, the diacetylene multi-layer is formed into a thick film by self-assembly. To disperse the diacetylene film dried in the crystalline form into the vesicle form in an aqueous solution, it is necessary to apply additional energy to impart the fluidity of the film. Membranes with sufficient fluidity above the melting temperature (T_m) of lipids are suspended in an aqueous solution and homogenized by sonication. Finally, after undergoing the recrystallization process at a low temperature, PDA vesicles can be generated by UV irradiation. Since the diacetylene vesicles can be photopolymerized *in situ* by UV irradation, the large quantity preparation of the suspension-type PDA vesicle is relatively easy.

The liposome-based PDA sensor is attractive for use as a sensor for biomolecule detection, due to its optical properties and accessibility of solution-based vesicles (Cho et al., 2016a; Kim et al., 2017b; Zhang

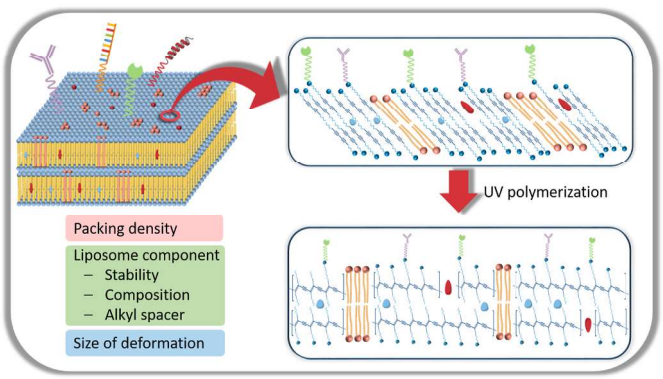

Fig. 5. Several Factors affecting the sensitivity and selectivity of PDA sensors in the self-assembly structure of diacetylene.

et al., 2018b). The liposome PDA sensor can be used by adjusting the amount of the solution according to the measurement equipment environment, sample volume, and sample concentration without any additional substrate. To use the PDA vesicle as a sensing application, receptors on the surface of the vesicle that allow ligand-receptor interaction with specific target substances must be introduced (Charych et al., 1993; Cho and Ahn 2013a; Lee et al., 2009b; Wu et al., 2012). However, depending on the substances added during the reaction for introducing receptors, PDA vesicles dispersed in an aqueous solution may aggregate or precipitate in a high concentration of salt or a non-neutral pH. Additionally, further processes are required to remove residual reactive chemicals and unbounded receptors (de Oliveira et al., 2015). For example, most unmodified PDA vesicles are stably suspended in distilled water, but precipitation can occur in salt-containing environments. Since not only salt but also proteins, such as albumin protein can precipitate PDA vesicles, this phenomenon must be considered for use in PDA vesicle-based biosensors, especially for biological buffer-based samples. To prevent sedimentation or aggregation of vesicles during the reaction process for the introduction of receptors on the PDA vesicle, PDA vesicles containing receptors can be prepared by mixing diacetylene-receptor molecules bound at the monomer level with monomeric diacetylene before vesicle formation (Lee et al., 2008). In this case, since the function of the receptor must be maintained even at a relatively high temperature during vesicle formation, a relatively stable aptamer is preferred over an antibody that undergoes irreversible denaturation at high temperature (Kim et al., 2020b; Lee et al. 2008, 2009b).

To improve the shortcomings of the vesicle itself, occurring in aqueous solution, a method of fixing the PDA vesicle to a 2D substrate has been proposed (Kim et al. 2003b, 2005b). The PDA vesicle fixed to the substrate is free from aggregation or sedimentation problems and is advantageous for quantification according to signal strength. Vesicles can be fixed covalently or non-covalently on a 2D plane or encapsulation can be performed with a 3D matrix (Li et al., 2015b; Yapor et al., 2017). The PDA vesicle immobilization method, which is widely used in sensor applications, is patterned using a mask or microarray (Jung et al., 2016; Nguyen et al., 2019; Park et al., 2016a). Since most sensor applications deal with various ions or molecules such as proteins, they can escape some precipitation problems that can be caused in these environments. In addition, PDA vesicles that are immobilized on a flat surface through microarrays can not only detect a small amount of sample, but also have the advantage of increasing the detection sensitivity of PDA vesicles through fluorescence observation (Zhang et al., 2016a). Diacetylene vesicles can be immobilized by covalent bonding mainly through EDC/NHS coupling (Lee et al., 2009b; Won and Sim 2012), aldehyde/-amine Schiff base (Kim et al. 2003a, 2005b), maleimide/thiol chemistry and others (Kang et al., 2017; Lee et al., 2008; Seo et al., 2013).

2.3.3. Other colloid structures

Initial studies of phospholipids dispersed in aqueous solutions did not deviate from the liposome structures of single or multiple bilayers. Lecithins, a type of phospholipid, have not changed the topology of liposomes in the synthesized form as well as the natural state (Evans and Kwok 1982; Inoko and Mitsui 1978; Yager et al., 1982). Meanwhile, attempts have been made to form a robust membrane through polymerization by introducing diacetylenic groups into lipids to create a more robust and stable lipid vesicle (Yager and Schoen 1984). In this process, it was found that polymerizable lecithin with diacetylene groups accompanied a phase transition from vesicle to cylinder-shaped tubules in case of temperature change (Yager et al., 1985). After this discovery, various types of non-spherical diacetylene assemblies such as tubes (Oh et al., 2016), helix (Meng et al., 2017), and ribbons (Li et al., 2017a) were found and bolaamphiphilic diacetylene molecules with numerous types of structures were developed (Cheng et al., 2000; Gravel et al., 2012; Song et al., 2004; Wang and Hollingsworth 2000; Xu et al., 2014b).

The assembly of amphiphilic molecules can appear in various forms and the chirality of the molecule is one of the factors that can influence the structure or shape of the assemblies (Schnur et al., 1994b). Therefore, since tubules or helices are assembled, it was thought that the topological chirality of PDA assemblies was based on the chirality of the diacetylene molecules in the early days (Schnur et al., 1994a). However, it has been described that the chirality of the molecule is not essential for the formation of the chiral tubule structure, as lecithin-based diacetylene monomers have achiral properties and form tubule assemblies (Lee et al., 2004; Pakhomov et al., 2003b). In addition, achiral diacetylene amine with hydrobromide salt in aqueous solution can also form colloids with non-spherical structures such as tubes, helices, and ribbons (Pakhomov et al., 2003a; Seo et al., 2015).

Recently, 1D materials, such as wires and tubules, have become promising material structures in fields such as photonics and electronics, as well as sensor applications (Chen et al., 2016; Li et al., 2017b; Yang et al., 2014b). In particular, it can be applied in optoelectronics because of its unique optical properties that can appear at sub-micrometer scales when dispersed in aqueous solutions (Xia et al., 2014). The non-spherical structure commonly found in PDA structures is in the form of a tube. This is derived from the film of the membrane and a wide plate is joined in the form of a pipe, producing up to a dozen micrometer-scale hollow tubes (Hu et al., 2014; Jiang and Jelinek 2016). Additionally, a PDA tube with a molecular level scale can be prepared using a circular diacetylene monomer. The PDA nanotubes formed by the self-assembly of nanotubes showed a higher tilt angle than PDA composed of normal linear monomers (Heo et al., 2017). Most PDA assemblies such as films or vesicles exhibit the optical properties of PDA (Johnston et al., 1980; Lin et al., 1982) and can be aggregated by external environments like other colloid structures (Reppy and Pindzola 2007b).

3. Sensitivity determination elements

From a biological point of view, molecular recognition or signal transduction at the cell surface is mainly caused by glycosylated lipids or proteins optimized through a long evolutionary process. These elements are involved in several important biological phenomena in the cell by recognizing specific motifs (Okada et al., 1998). Early strategies of biosensors imitated an artificial membrane with the characteristics of a bio-membrane capable of recognizing a specific molecule (Katrlik et al., 1996; Peter et al., 1996; Reshetilov et al., 1997). Due to efforts to find a more stable and stronger polymerizable membrane, PDA vesicles resembled the structural and functional properties of plasma membranes with high stability. For PDA to act as a sensory material for specific analyte detection, the DA molecule should be a membrane or film structure. The assembled diacetylene aggregates convert into PDA through polymerization by UV irradiation. When an external stimulus is applied to the PDA membrane, disturbance of the conjugated bond inside the PDA occurs and the optical properties of PDA change (Carpick et al., 2004; Dobrosavljevic and Stratt 1987). Like other materials, PDA can also possess various properties depending on the composition and the components that make up the supramolecules. The conjugated bond inside the PDA can increase or decrease the degree of change by several factors constituting the PDA (Kuriyama et al., 1996b; Lio et al. 1996, 1997; Mino et al., 1991; Tomioka et al., 1989). Monomer distance affects UV-induced polymerization and liposome stability, lipid composition, alkyl spacer, and lipid size can also be factors affecting the sensitivity of PDA vesicles (Fig. 5).

3.1. Packing density (assembly distance) and topochemical structure

Amphiphilic lipid monomers can assemble diacetylene aggregates through self-assembly and can induce *in situ* polymerization by UV irradiation at a wavelength of 254 nm. For intermolecular 1,4-addition to occur efficiently under UV irradiation among adjacent diyne groups, appropriate distance and spatial arrangement of diacetylene monomers

is required (Vizgert et al., 1989). The ideal arrangement of solid-state diacetylenes is an intermolecular distance of 5 Å, at tilting angle of 45°, and a distance between C1 in one monomer, and C4 in the adjacent diacetylene monomer of 3.5 Å (Baughman 1972) (Fig. 1b). Nevertheless, depending on the structure or morphology of the DA monomers, the assembly patterns and conditions for favorable polymerization can vary widely. In the case of a diacetylene monomer with a linear alkyl chain, the distance between the monomers in the polymerized PDA is 3.7 nm, and the distance of the basic diacetylene monomer can induce polymerization in a stable form at 4.5 nm. If the gap between monomers is too wide or too narrow, the efficiency of polymerization dramatically decreases or disturbance of the conjugated bond formed by unstable polymerization results in unusual color transitions such as purple, pink, and orange after polymerization (Okada et al., 1998). The polymerization efficiency can be affected not only by the distance between monomers but also by the spatial arrangement of adjacent diynes. In particular, the efficiency of polymerization may drastically decrease or polymerization may not be possible when self-assembly is performed by a substrate, such as a gold film or particle. For example, SAM diacetylene monomers with a higher tail length on a gold surface are favorable for the arrangement of diacetylene molecules. The aligned arrangement increases the crystallinity of the SAM and shows a high degree of polymerization efficiency. However, in a situation where one side is fixed to the surface, the arranged triple bonds form a suitable angle for hybridization. As the diacetylene group is closer to the head group, a stable film is formed as the collapse pressure increases on the surface of the diacetylene assembly. However, the PDA formed by polymerization has a red or yellow color rather than a normal blue color.

More precisely, as the length of the alkyl spacer of the head group of the diacetylene monomer decreases, the polymerized PDA color in its initial state gradually shifts from blue to red and the PDA with the shortest spacer appears yellow during polymerization. The suitability of polymerization is also affected by the tilting angle during diacetylene assembly. When the tilting angle of diacetylene shows a value around 45°, it shows the normal blue-red transition state, while the PDA shows a red state below 20° and a yellow state above 65° (Khanantong et al., 2018; Tachibana et al., 1999).

3.2. The nature of the liposome component

As a sensor material, the PDA membrane structure began to be present in the process of mimicking the intracellular plasma membrane, and it has similar properties to those of the intracellular plasma membrane (Kunitake and Okahata 1977). For example, because the element that determines the fluidity of the plasma membrane is similar to the element that determines the monomer fluidity in the PDA vesicle, the fluidity of the PDA membrane can be modulated by introducing elements that can be involved in the PDA membrane (Mapazi et al., 2018; Park et al., 2016b).

3.2.1. Stability of liposome formation

The membrane stability of PDA is determined by the degree of self-assembly and greatly influences the polymerization efficiency in LB films or SAM assemblies. PDA films fabricated using this technique affect factors such as thermal stability, uniform surface density, and film area. If the systematically arranged structure meets the ideal topochemical structure for polymerization, a relatively high level of polymerization can be achieved, resulting in a clear color change. For example, when two of the most widely used diacetylene monomers, 10,12-tricosadiyonic acid (TCDA) and PCDA liposomes, were exposed to UV for polymerization under the same conditions, PCDA exhibited higher absorbance due to UV polymerization. Since PCDA with a relatively long alkyl group forms a more stable membrane, it means that PCDA is more advantageous in forming a membrane structure.

In general, polymerized PDA films are more stable than diacetylene assembled films and show improved packing through annealing at elevated temperatures before polymerization. When manufacturing the LS film, nitrogen flow is provided at the liquid–air boundary and a very uniform film can be produced through the heated substrate. Additionally, the presence of divalent cations, such as Ca2+ or Cd2+, plays a role in enhancing the stability of the carboxylic acid-based diacetylene film.

Some diacetylene monomer layers are so stable that they can reverse the color change of irreversible PDA (Ahn et al., 2009; Khanantong et al., 2020; Lee et al., 2014c). To increase the stability of the diacetylene layers, a method of increasing the interaction between diacetylene molecules is used. First, hydrogen bonds between molecules can be imparted. When a group such as an amide bond is introduced into the diacetylene monomer chain, an intermolecular interaction is additionally generated by hydrogen bonding between molecules. In addition, when a phenyl group is present at the molecular end, the accumulation of molecules may be promoted by the π-π stacking of electrons located in the benzene ring. Finally, diacetylene is anchored to the surface of the inorganic material, so that stable diacetylene layers can return to their original shape even after distracting (Wu et al., 2018). PDA films consisting of diacetylene monomers with these properties are resistant to color change caused by excessive UV irradiation or organic solvents, and cause color changes at higher temperatures (Hong et al., 2015; Park et al., 2014).

3.2.2. Composition of lipids

Diacetylene monomers, which have the structural properties of common lipids, have an alkyl chain in both directions around the diyne with a hydrophilic group at one or both ends. Depending on the number of alkyl groups, a wide variety of diacetylene vesicles can be produced. Additionally, various types of diacetylene monomers can be constructed instead of one type of diacetylene monomer (Cho and Ahn 2013b; Khanantong et al., 2018). This uses the lipid properties of diacetylene, and suitable diacetylene monomers can be applied depending on the application.

3.2.3. Alkyl spacer

In the general form of the DA monomer, a spacer connects the tail and head groups of the alkyl form around diyne. DA or PDA assemblies have different responsive properties depending on the number of alkyl groups of tails or spacers. To manufacture a PDA sensor that responds to a specific signal, a method of introducing a receptor on the PDA membrane surface has been used. When a new interaction occurs with the ligand of the receptor on the PDA surface, the generated stimulus is transferred from the surface of the PDA to the conjugated backbone. At this point, the alkyl spacer between the backbone and the surface of the PDA with the receptor plays a role in transmitting the stimulus generated by the interaction. In general cases, the PDA sensitivity may increase as the alkyl spacer becomes shorter (Khanantong et al., 2018; Potai et al., 2018). However, in the case of too short spacer, a trade-off exists in which the assembly of monomers is poor, resulting in low polymerization efficiency (Charoenthai et al., 2011; Seo and Kim 2010). A long spacer increases the degree of freedom of the diacetylene terminal so that the generation or delivery of stimuli by interaction is not effectively achieved.

In the case of general carboxylic diacetylene, the physical and self-assembly properties of PDA vary depending on the alkyl length of the head and tail. As the alkyl tail length decreases, the intermolecular force weakens, due to the hydrophobic effect, and the T_m of the diacetylene crystal decreases. On the contrary, as the alkyl length of the head portion become shorter, the T_m increases rapidly because the charge of the head group creates hydrogen bonds during crystal formation. As the length of the alkyl spacer of the head group decreases, the tilting angle of the DA assemblies in the crystal form increases. The alkyl spacer and the tilting angle in the crystal form are factors that determine the size of vesicle assemblies.

The colorimetric behavior of PDA assemblies in aqueous suspensions corresponds to the stability of diacetylene crystals. For example, the

PDA membrane with the shortest alkyl chain in the head group shows the highest color change transition temperature. Also, color change significantly was reduced when PDA assemblies are exposed to chemical stimuli, such as organic solvents and pH environments because of the difference in the mechanism that causes the color conversion of the PDA membrane (Khanantong et al., 2018).

3.3. Size of deformation

PDA liposome vesicles can be manufactured in a wide range of sizes from dozens of nanometers to several microns, through different production methods (Pevzner et al., 2008). Vesicles, even those with the same lipid composition, generated from one sample have various size distributions. Depending on the size or shape of the vesicle, the structural characteristics of the diacetylene monomer and the spatial arrangement can affect the sensitivity of the PDA vesicles (Nopwinyuwong et al., 2014; Peek et al., 1994). Under the same conditions, the smaller the liposome size, the more sensitive it tends to be, which is expected to increase the sensitivity of PDA by increasing the steric hindrance generated by the target molecules (Baek et al., 2016; Peek et al., 1994). The size of the liposomes also varies depending on the structure and properties of the lipids that make up the membrane. In the DA, as the length of the head spacer becomes shorter, the size of the resulting liposomes gradually increases resulting in, a rod-like structure with a spherical shape (Khanantong et al., 2018).

4. Signal enhancement strategies of PDA sensor platform

The unique optical properties and customizable features of PDA serve as an advantage for sensor applications, but one of the drawbacks of PDA is the difficulty in detecting trace target molecules because of their relatively low quantum yield (Lecuiller et al., 1999; Olmsted and Strand 1983). Considering that, as a sensor material, high sensitivity and reliability are required in a wide range of fields, it is necessary to amplify the PDA signal. Since the PDA signal occurs in proportion to the degree of structural distortion of the conjugated bond of the backbone, strategies to significantly change the backbone of the PDA through various methods have been studied (Fig. 6). By improving the sensitivity of PDA sensors, it can be applied to detect low concentrations of target molecules, and it can be extended to a wide range of applications such as food freshness testing or disease diagnosis.

4.1. Impurities

The vesicle of the PDA bilayer was proposed to mimic the plasma membrane of the cell (Okada et al., 1998). Since the structural properties of PDA monomers are similar to those of the lipids that make up the membrane, there are similarities to those of the plasma membranes. The plasma membrane is a fluidic membrane composed of a basic phospholipid bilayer as the main component, in which numerous types of proteins are embedded, called a fluid mosaic model. Polymerized diacetylenes have a solid form of properties, having a glass transition temperature that begins to flow above a certain temperature. The characteristics of PDA are determined according to the alkyl chain and hydrophilic groups of the diacetylene monomer constituting the PDA membrane.

Similar to the cell membrane, including the type of diacetylene constituting the PDA liposome, the sensitivity of PDA can be changed by lipids or cholesterol. Amphiphilic lipid molecules, such as surfactants (Shin et al. 2015, 2017) or phospholipids (Kang et al., 2012b; Kim and Lee 2019; Kim et al., 2008; Kolusheva et al., 2008), with similar properties to diacetylenes are frequently used, and impurities, such as cholesterol, are used with lipid molecules (Fig. 7) (Kolusheva et al. 2000b, 2003; Kwon et al., 2014). Since the added impurities are co-assembled with diacetylene molecules in the liposome formation step, they flow between the alkyl chains of diacetylene. However, the impurities in diacetylene assemblies form a separate domain or are trapped in the diacetylene chains because diacetylene has a rigid structure through polymerization. The impurities present in the lipid bilayer change the degree of freedom of the DA alkyl chain and affect the mixed membrane structure fluidity. The PDA membrane with increased fluidity or relative isolation can be more or less sensitive to external signals or stimuli, achieving a lower limit of detection (LOD) for the PDA sensor. The higher the compositional ratio of impurities added, the more impurities contribute to the change in the sensitivity of the PDA liposome. However, the formation of liposomes becomes impossible above a certain ratio of impurities (Kang et al., 2012b; Kim et al., 2008; Su et al., 2004).

4.2. Secondary interaction

Sensors for the detection of specific substances have developed using various principles in a wide range of fields. In these various types of detection methods, many studies are being conducted to improve the

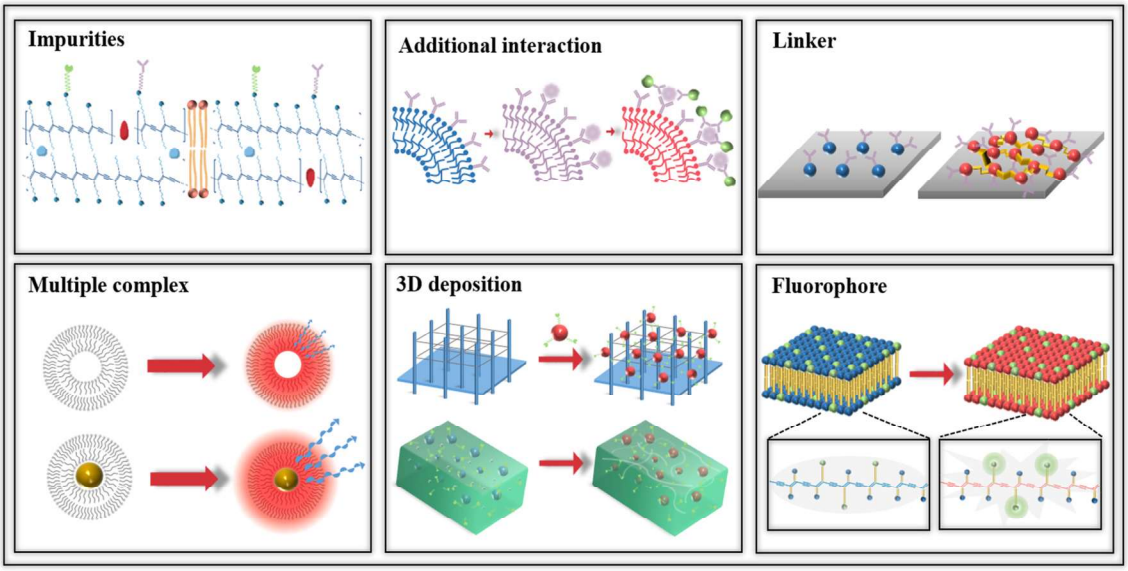

Fig. 6. Schemtic illustration of several strategies to improve the sensitivity of polydiacetylene based sensor.

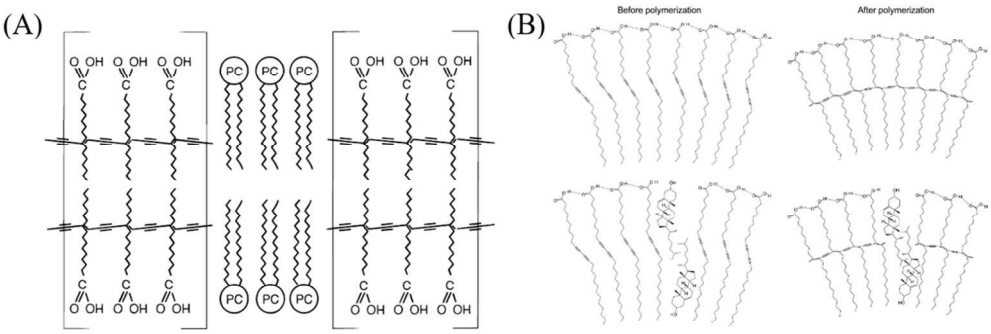

Fig. 7. First strategy to improve the sensitivity of polydiacetylene based sensors: Increased fluidity of PDA membranes by mixing PDA monomer with impurities. Illustration of domain separation between two constituents that appears when polymerization is performed after forming a membrane in case of (A) phospholipid or (B) inserted cholesterol in the PDA membrane. This Section adapted with permission from ref (Kolusheva et al., 2000b). Copyright 2000, American Chemical Society and (Kwon et al., 2014). Copyright 2014, Korea Chemical Society.

accuracy of the sensors and to detect a target substance, even at low concentrations. Following these efforts, many technologies have been developed to improve the sensitivity and accuracy of PDA-based sensors. There are two methods of improving the performance of a PDA-based sensor, namely, increasing the stimulus provided to the PDA or amplifying the optical properties of the PDA itself. Depending on the substance detection mechanism, the intensity of the primary reaction is considerably small, making it impossible to detect the target substance at low target concentrations. In this case, it is possible to overcome the low concentration target environment by applying additional stimulation to the PDA. The second method implies the performance improvement of the sensor by improving the optical features of the PDA itself. Therefore, it is necessary to amplify the signal generated in the primary stimulus and overcome the limitations of the signal detection method.

4.2.1. *Nanoparticle-based interaction*

The target detection of the PDA-based sensor system using receptors is usually derived from ligand-receptor interactions. Ligand-receptor interactions occurring in living organisms are widely adopted in sensor applications because they usually interact and detect the target substance with high specificity. At low target substance concentrations, it remains sparsely bound to the liposome, whereas at high target substance concentrations, it binds tightly to the PDA surface by the ligand-receptor. When the PDA surface is filled with a ligand, the repulsion force by steric hindrance is induced (Seo et al., 2013). The repulsion force generated at this step is transmitted to the PDA backbone and induces color changes. Since this process occurs at the nanometer scale, efforts have been made to apply substitutes with similar size scales. Among the numerous methods, it is possible to induce the signal amplification of PDA by performing a secondary reaction with nanoparticles. Additional hindrance can be added to the primary signal generated by the first binding by using specially modified nanoparticles. For nanoparticles to have the ability to attach to a specific analyte, a method of introducing a receptor on the surface of the nanoparticles is possible. The material or shape of the nanoparticles used can be prepared in various ways depending on the purpose. After the first ligand-receptor reaction occurs, the addition of nanoparticles to generate additional stimuli can increase the signal of the PDA, leading to the increased sensitivity of the PDA sensor system (Kwon et al. 2010, 2012). That is, these receptor-functionalized nanoparticles can act as pseudo-analytes by interacting with the analyte bound to the PDA surface after the first interaction.

For example, in a PDA microarray system for detecting human immunoglobulin (hIgE), gold nanoparticles functionalized with a polyclonal antibody were applied onto a PDA array that was primarily modified by a target molecule. The added nanoparticles were bonded to the target protein interacting with the PDA vesicle and provided additional repulsion force to the PDA vesicles (Won and Sim 2012). The larger the gold nanoparticles applied, the more repulsive power it could generate, resulting in more deformation of the PDA. Through the addition of functionalized nanoparticles, the LOD of the arrayed PDA improved to about 100-fold. Another method used iron nanoparticles functionalized with antibodies of the prostate-specific antigen, and these nanoparticles created a secondary reaction due to the repulsive physical force in the PDA array with the primary strain (Kwon et al., 2012). By applying a magnetic field of alternating current in both directions, a physical vibration was additionally applied to the paramagnetic iron nanoparticle, applying a third stimulus to the PDA vesicles. With the introduction of functionalized nanoparticles, a detection limit of 0.01 ng/mL could be achieved. The introduction of such nanoparticles can be widely used as a strategy to increase the PDA deformation by inducing additional repulsion of PDA vesicles.

4.2.2. *Polyclonal receptors*

Unlike molecules with low molecular weights, macromolecules, such as proteins, often have multiple specific sites that can be recognized by polyclonal antibodies. In this case, more recognition sites can be obtained from the same amount of analyte than when using a monoclonal antibody that can recognize only one site. As the number of recognition sites increases, the ability to interact with the PDA vesicle becomes larger. Naturally, the higher level of interaction allows the PDA vesicles to have a higher sensitivity. To detect a molecule or protein with multiple recognition sites, multiple receptors can be adopted in one liposome system, thereby increasing target binding capacity (Jung et al., 2010). This is one of the advantages of PDA where multiple receptors can be introduced on one PDA membrane platform (Lee and Kim 2012). The researchers in this work used two types of aptamers for each site to detect thrombin with two distinct recognition sites. Each aptamer was bound to the DA monomer before vesicle formation and mixed with the basic DA monomer to form a PDA vesicle with multiple aptamers (Fig. 8a). At the same thrombin concentration, PDA liposomes with a single aptamer exhibited a blue to purple color change, whereas PDA liposomes with multiple aptamers exhibited a blue to red color change. That is, the CR value was greater than that observed with the naked eye of the liposome with one receptor.

4.2.3. *Enzyme-linked secondary response*

Signal transduction or metabolic systems in living organisms maximize the response to be achieved through multi-dimensional responses. To detect small reactions or signals that can occur *in vivo*, signals are amplified through each step of consecutive intermediate reactions. Enzyme-linked immunosorbent assay (ELISA) is a representative detection assay that uses an enzyme reaction. ELISA can detect a small amount of target proteins or molecules through the second reaction or more and they add a flow over time as a reaction by an enzyme (horseradish peroxidase, HRP) to provide fast and intuitive results. Because of this phenomenon, secondary reactions have been widely used as a strategy to amplify molecular signals by introducing substances that act as catalysts (Lim et al., 2019; Park et al., 2016c). Catalysts or enzymes can cause durable and cascading reactions in sensor applications to amplify the final products. That is, by applying the

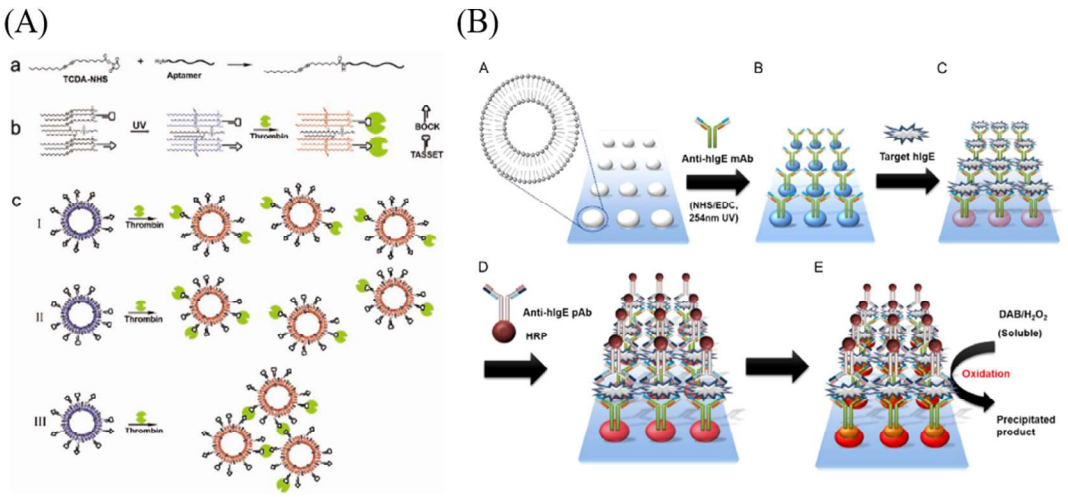

Fig. 8. Second strategy to improve the sensitivity of polydiacetylene based sensors: Improving the sensitivity of PDA by adding additional stimuli such as secondary interactions to the PDA. (A) Schematic illustration of the process of inducing additional interaction using dual aptamers for thrombin detection system. (B) A scheme showing the process using HRP-Ab composite to improve the detection sensitivity of the microarray platform. This Figure reproduced with permission from ref. (Jung et al., 2010). Copyright 2010, WILEY-VCH Verlag GmbH & Co. KGaA, Weinheim. and (Lee et al., 2014b). Copyright 2014, Elsevier B.V.

phenomenon with enzymes to the PDA-based sensor, the detection performance of PDA can be increased by eliciting an additional reaction. A secondary polyclonal antibody can be attached to the target molecules captured by the PDA vesicles. If a polyclonal antibody has a catalyst that enables a secondary reaction such as HRP, additional modification of the PDA is possible owing to the secondary reaction of the catalyst (Fig. 8b). Through this process, advanced PDA sensor systems can be built as a more sensitive sensor due to an additional response to the PDA (Lee et al., 2014b).

4.3. PDA complex

4.3.1. Introducing inter-linkers

PDA vesicle-based platforms functionalized with a receptor are mainly used in the PDA sensor field because of its easy handling and versatility. In particular, in the case of the PDA vesicles dispersed in an aqueous solution state, the signal can be measured simply by mixing with a sample. However, a relatively large amount of sample is required to measure the colorimetric change or fluorescence intensity of a PDA dispersed in an aqueous solution. If the sample size is small or the concentration of the target substance is very low, detection in aqueous solution may not be suitable because of the low analytes to PDA vesicles ratio. To prepare a PDA sensor that can be analyzed even with a small amount of sample, a microarray method in which a PDA vesicle is immobilized on a 2D substrate was introduced (Kang et al., 2017; Kim et al., 2003a). Although the number of immobilized vesicles composed of one vesicle layer through the microarray was much smaller than the vesicles dispersed in the solution, signal analysis was possible through fluorescence measurement. It has the advantage of measuring small or low concentration samples owing to the limited number of vesicles, so it is used as a typical signal increase method for PDA-based biosensors. Also, when the detection material is fixed on the substrate, signal detection from the sensing materials can be performed in a gradually concentrated environment while evaporating the solution containing the target material (Wang et al., 2018b). However, since it is difficult for the PDA vesicles which are immobilized on the substrate to exist as a dense layer, a method of increasing the density of the PDA vesicle immobilized through the inter-linker between the vesicles was used. PDA vesicles existing in 2D substrates can be expanded to 2.5D to obtain aggregated vesicles or PDA vesicles with several layers (Choi et al., 2011; Kim et al., 2011; Park et al., 2009). By introducing the inter-linker, the fluorescence signal of the PDA vesicle can be obtained more effectively.

For example, to further enhance the immobilization of PDA vesicles, diamine was introduced to form bundles of PDA vesicles exhibiting increased surface immobilization as compared to individual PDA vesicles (Fig. 9a). The bundle of PDA vesicles could be densely immobilized than a single vesicle, and through high integration, this group developed a platform that could obtain the fluorescence signals in excess of ten-fold stronger. By forming a group of vesicle complexes, it is possible to increase the signal generated from the PDA while maintaining the selectivity of the PDA (Park et al., 2009). Alternatively, avidin was introduced on the surface of the PDA to create a multilayer of PDA vesicles through the layer-by-layer method by avidin-biotin or electrostatic interaction (Fig. 9b). The PDA fluorescence signal was enhanced as the number of layers increased due to the vesicle stack (Choi et al., 2011; Kim et al., 2017a).

4.3.2. Nanoparticles-PDA liposome complex

The fluorescence-based platform is a widely used spectrum technology in a wide range of fields, including chemosensors for biosensor applications (de Silva et al., 1997; Thomas et al., 2007). Fluorescence analysis technology is a promising method for sensing applications because of its sensitivity, simplicity, non-invasiveness and multiplex detection of analytes (Ai et al., 2008; Jeong et al., 2018). As the field of fluorescence technology is gradually widening, fundamental methods to increase fluorescence signal have gradually emerged. In particular, several physical phenomena, such as fluorescence efficiency, autofluorescence, quenching and photobleaching of the fluorophore, are usually considered in fluorescence-based sensor applications. Since the sensitivity of the fluorescence platform applied in the biosensor or chemosensor is a crucial element, these phenomena related to fluorescence have become an important criterion for high fluorescence intensity and photostability of the fluorophore (Hacia et al., 1996; Nguyen-Ngoc and Tran-Minh 2007). PDA is also considered as a potential fluorophore, but its low quantum efficiency is one of its major disadvantage. For this reason, research on platforms that can improve the quantum efficiency of PDA for PDA-based sensor applications is ongoing. Among several platforms, the method using metal structures and nanometer-scale particles is used as an effective method to improve fluorophore fluorescence performance. This phenomenon is called metal-enhanced fluorescence (MEF) and when nanometer-scale metal particles maintain an appropriate distance from the fluorophore, the fluorescence amplification effect of the fluorophore is based on plasma

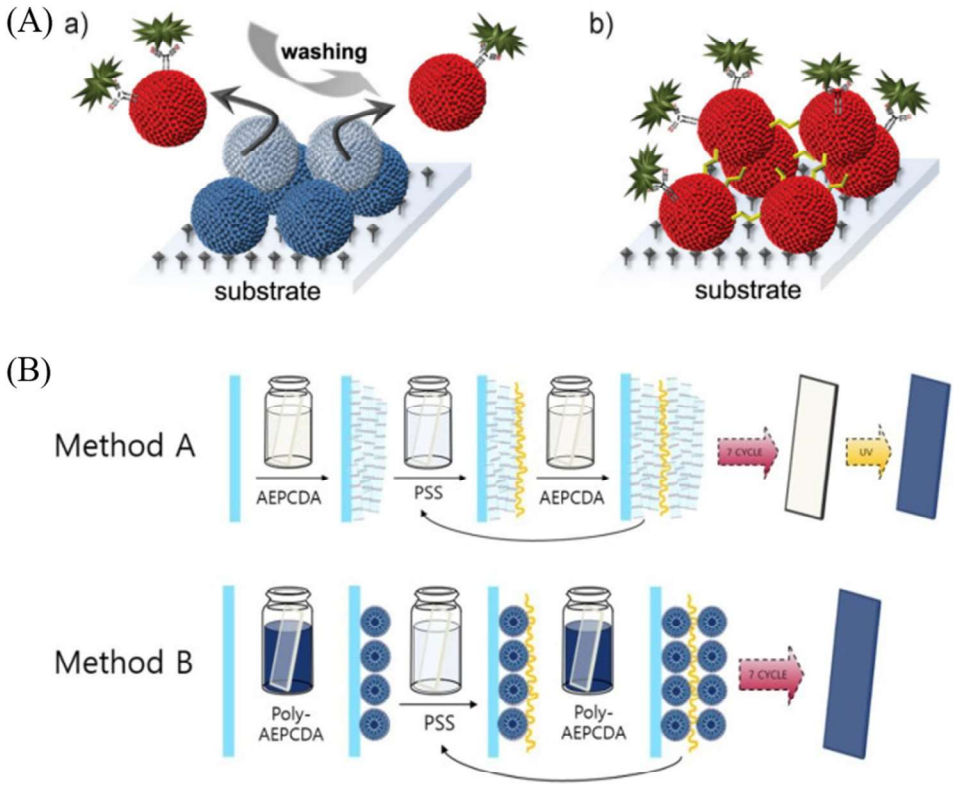

Fig. 9. Third strategy to improve the sensitivity of polydiacetylene based sensors: (A) Comparison of existing PDA vesicle array and PDA vesicle array with interlinker. (B) Multilayer polydiacetylene membrane lamination through layer-by-layer technique. These figures reproduced with permission from ref. (Kim et al., 2020b). Copyright 2020, Licensee MDPI and (Kim et al., 2017a) Copyright 2017, WILEY-VCH Verlag GmbH & Co. KGaA, Weinheim.

coupling. By using these fluorescence amplification phenomena, various sensor applications increase the sensitivity of fluorescence and help to detect substances with lower concentrations (Jeong et al., 2018; Wang et al., 2018b). A simple way to introduce metal nanoparticles into PDA is to form a PDA membrane around the metal particles. If the diacetylene monomer is wrapped around metal nanoparticles to form a core-shell structure, the distance between the PDA backbone and the metal particles can be kept constant due to the alkyl chain of the spacer or tail. The preparation of PDA-metal nanoparticle composites is largely classified into three methods, namely, incubation to replace the polysaccharide stabilizer with diacetylene (Alloisio et al., 2015), hydrothermally coating diacetylene dispersed in an aqueous solution at high temperature (Cui et al., 2018), and the microwaving method to surround diacetylene on the surface of metal particles using instantaneous heat (Yokoyama et al., 2009). Due to the interaction with metal nanoparticles, PDA composites with metal nanoparticle cores can emit amplified fluorescence signals more than ordinary PDA vesicles without metal nanoparticle cores (Cui et al., 2018). For example, a sensor system was designed to detect probe DNA by forming PDA-AgNP shell-core composites (Fig. 10a). Owing to the introduction of AgNP, simultaneous Raman scattering and photoluminescence (PL) increased, with the Raman signal increasing in excess of 100-fold and the LOD for the target DNA could be achieved to 100 amol (Kim et al., 2020b). Furthermore, by forming a PDA shell around the metal nanoparticles and the particles to which the raman material is attached for SERS, the change in the raman signal due to the PDA deformation can be greatly amplified (Kim et al., 2015a) (Fig. 10b). However, the MEF or Raman amplification can be sensitive to distance, so a detailed optimization process where a spacer that maintains a proper distance between the metal nanoparticles and the PDA, is additionally required.

4.4. 3D deposition or encapsulation of PDA liposomes

Since the first membrane-based PDA-based sensors were developed, PDA-based biosensors have mainly use liposomes dispersed in aqueous solutions or 2D structures such as microarrays. Because the 2D microarray can only observe a few layers of liposome, it is difficult to obtain sufficient signal strength for observation. To overcome the intrinsic limitations of the 2D format, a method of introducing a network of 3D PDA liposomes was proposed. The 3D network, created by adding the height dimension to the existing 2D plane, can increase the number of PDA vesicle layers capable of performing signal observation, enabling a PDA liposome sensor with high sensitivity at a lower concentration target. For example, a carbon nanotube with uniformly spaced pillars was formed on a silicon substrate and cross-linked to the pillars, forming a 3D network frame. When comparing the alpha-cyclodextrin detection limit of a typical 2D PDA vesicle and a PDA vesicle immobilized in a 3D frame, by changing the structure it was possible to lower the LOD from the millimolar level to the micromolar level (Lee et al., 2016c) (Fig. 11a). Another 3D composition method used PDA-silica bead conjugates by attaching a functionalized PDA vesicle around a relatively hard silica bead. This conjugate exhibited a greater color change and fluorescence signal than conventional PDA vesicles dispersed in an aqueous solution, achieving the LOD of PET protein to 20 nM level (Lim et al., 2011).

Besides the 3D hard material framework, a method of wrapping PDA liposomes with another 3D material exists. The most widely used material for wrapping materials is hydrogel (Lee et al., 2011). The hydrogel can be easily prepared in an aqueous solution and is used as a material surrounding PDA because target molecules can easily enter and exit owing to their porous structure (Zhang and Khademhosseini 2017). For example, to detect genetically modified crops, polyethylene glycol-based hydrogels were formed on microfluids by encapsulating PDA vesicles modified with phosphinothricin acetyltransferase (PAT)

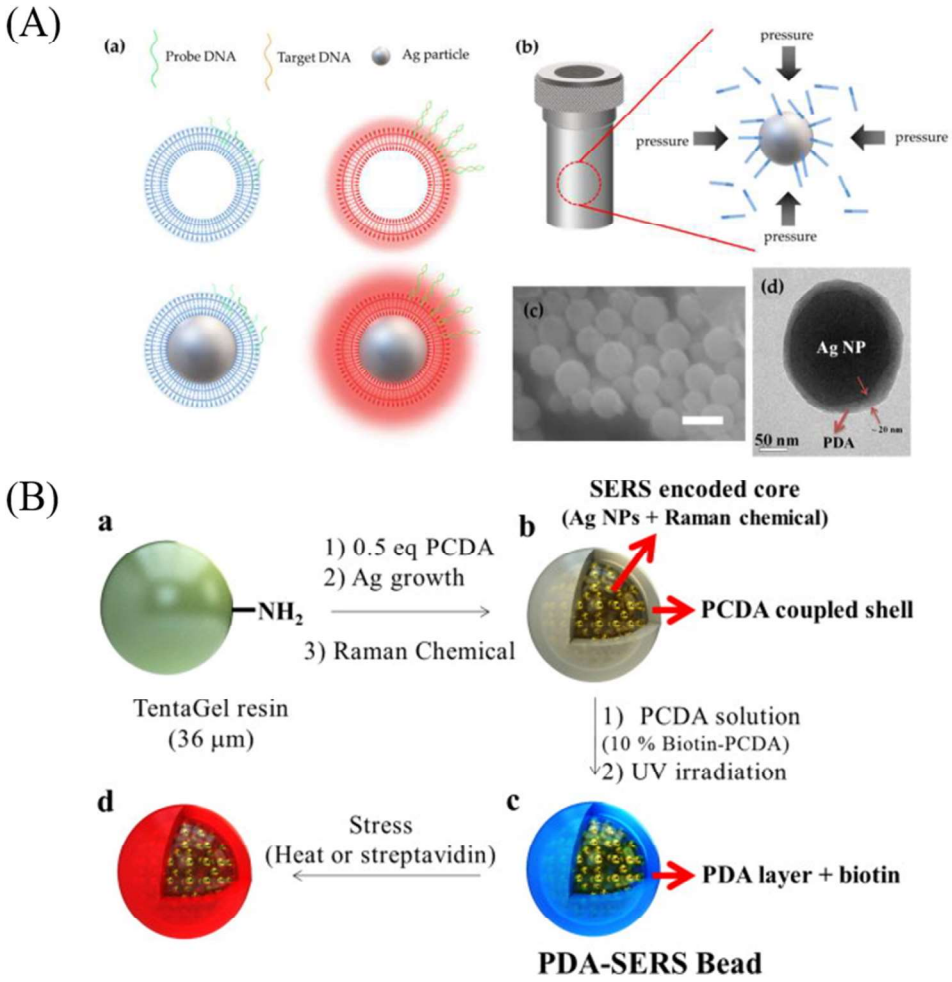

Fig. 10. Fourth strategy to improve the sensitivity of polydiacetylene based sensors: (A) Production process of AgNP-PDA core-shell composite made by PDA monomer coating through the hydrothermal process. (B) SERS encoded core encapsulated by PDA layer for the enhanced raman signal. These figures reproduced with permission from ref. (Park et al., 2009). Copyright 2009, WILEY-VCH Berlag GmbH & Co. KGaA, Weinheim and (Kim et al., 2015b) Copyright 2014, Elsevier B.V.

antibodies. Immuno-hydrogel beads changed color at significantly lower PAT concentration than PDA vesicles in aqueous solutions and lowered the LOD to approximately 10 nM (Lim et al., 2011). As another hydrogel material, alginate gel was wrapped in dopamine-functionalized PDA vesicles for the more sensitive detection of lead ions than the control group (Wang et al., 2015) (Fig. 11c). Similarly, microparticles surrounding multiple sensory PDA liposomes can be formed. The highly concentrated portion in the 3D space using the alginate hydrogel led to an improvement in sensitivity of about 20 times that of the lead ion, the target material, and the existing 2D PDA sensor platform (Fig. 11b). The method improved the sensitivity and enabled the simultaneous detection of multiple target substances using multiphase sensory PDA liposomes (Lee and Kim 2012).

4.5. Collaboration with fluorophores

Because a single PDA membrane has a relatively low quantum yield, the repulsive force due to the low concentration of the target substance may not be sufficient to cause the PDA backbone to deform (Olmsted and Strand 1983; Reppy and Pindzola 2007b; Wang et al., 2016). In particular, when the colorimetric or fluorescence signal of PDA in the aqueous solution is weak, signal analysis of the PDA may be unsatisfactory because the conjugated bond constituting the PDA backbone acts as a trap state of the electron to induce non-radiative relaxation emission. To supplement the low fluorescence efficiency of the disturbed PDA, a method to introduce new fluorescence fluorophores was proposed (Reppy and Pindzola 2007b). Since the PDA supramolecule is also a type of fluorophore, interactions between the fluorophores appear when a new fluorophore is introduced into PDA. The fluorophores used with PDA usually include organic molecules, inorganic materials (Dolai et al., 2017; Nopwinyuwong et al., 2014), metal nanoparticles (Dubas et al., 2017; Gu et al., 2020; He et al., 2020; Liffmann et al., 2015), and quantum dots (Kyeong et al., 2013). The auxiliary materials can be added as fluorescence, forming a composite with PDA to supplement or replace the insufficient fluorescence efficiency of PDA. Among them, Förster resonance energy transfer (FRET) is a typical phenomenon of interaction between fluorophores at a suitable distance. Since this phenomenon is highly sensitive to the distance between two fluorophores, it is used in sensor applications utilizing the interaction between two separated fluorophores (Charron and Zheng 2018; Chen et al. 2012a, 2019). It is used in various fluorescence-based fields due to its advantage of controlling fluorescence (Dubertret et al., 2001). PDA is also a type of potential fluorophore that can emit fluorescence under certain conditions and research has been conducted to use PDA using this phenomenon with other fluorophores (Kuroda and Swager 2003; Li et al., 2008; Ma et al., 2006). In the well-established blue state of PDA, the conjugated bond of PDA is an energy acceptor when the surrounding fluorophore is present. On the contrary, the modified conjugated bond in the red state cannot act as an energy acceptor for the fluorophore, so it can no longer quench the surrounding fluorophore (Ma et al., 2006). For

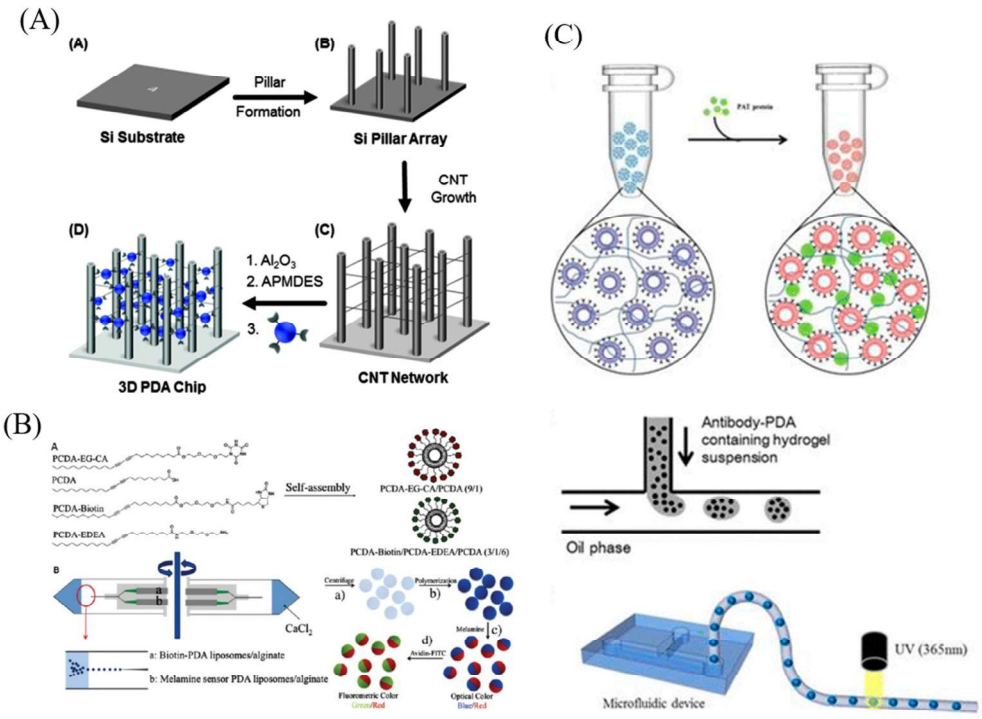

Fig. 11. Fifth strategy to improve the sensitivity of polydiacetylene based sensors: (A) Illustration showing the process of attaching PDA vesicles to a carbon nanotube-based framework. (B) Schematic illustration of alginate encapsulated PDA vesicle formation for melamine detection. (C) encapsulation of PDA vesicle in hydrogel using microfluidic device. Section A reproduced with permission from ref. (Lee et al., 2016c). Copyright 2016, The Royal Society of Chemistry. Section B reproduced with permission from ref. (Lee and Kim 2012). Copyright 2012, American Chemical Society. Section C adapted with permission (Jung et al., 2015).

example, researchers inserted a fluorophore dye between diacetylene monomers on the assembly membrane to form vesicles. In the blue state, the fluorophore was quenched by the adjacent conjugated bond and did not exhibit fluorescence. A reversible "turn-on" of fluorescence based on the ambient pH was possible by using the fluorescence quenching ability of the surrounding fluorophore by FRET of the conjugated bond (Ma et al., 2006). The PDA composites in this study did not focus on the color change of the PDA itself. It showed reversible quenching of the fluorophore according to the state of the conjugated bond that responded to changes in the surrounding pH environment.

In other study, a strategy was used to directly amplify the PDA fluorescence by FRET by connecting the dye directly to a DA monomer. The fluorescence dye, which acted as an energy donor, collected energy and transferred energy to the PDA liposome to amplify the fluorescence signal emitted by the PDA. The fluorescence amplification caused by the FRET phenomenon was affected not only by the ratio of the DA monomer and dye, but also by the length of the linker between the DA and dye, resulting in an 18-fold fluorescence amplification (Li et al., 2008). By introducting a highly fluorescent dye into the diacetylene monomer, Wang et al. proposed FRET-applied PDA vesicles which enabled the detection of lower concentrations of cationic surfactant in an aqueous solution than traditional PDA vesicles (Wang et al., 2016) (Fig. 12a). Fluorophore based method can also be used in the field of imaging for observing bacteria or cells by using the properties of the fluorophore to be introduced. Wu et al. developed a PDA vesicle system by mixing a ligand lipid capable of receiving bacterial lipopolysaccharide (LPS) and a lipid with a fluorescent dye in the DA monomer to develop a biosensor of the turn-on fluorescence signal. When the PDA vesicle bonded to LPS on the *E. coli* surface, the fluorophore quenched by the conjugated bond recovered the fluorescence (Wu et al., 2011a). In Fig. 12b, Wang et al. have created a sensor that can detect MUC1 expressed in cancer cells in an aqueous environment at 0.8 nM level by introducing MUC1-aptamer with Cy3-fluorophore into PDA vesicles. The fluorophore method has the advantage that the distance from the PDA backbone can be easily optimized through linker molecules (Wang et al., 2020).

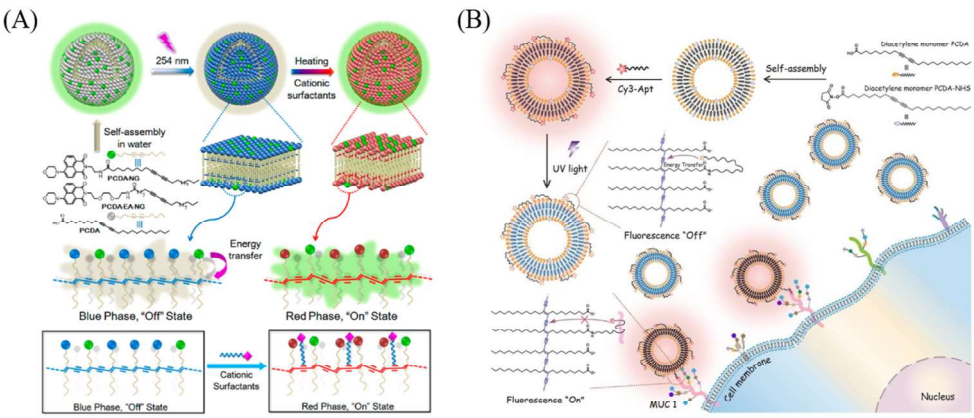

Fig. 12. Sixth strategy to improve the sensitivity of polydiacetylene based sensors: Introduce fluorophore to change the target of fluorescence from PDA to fluorophore to improve quantum efficiency. (A) Scheme illustration showing the formation of PDA vesicles with fluorophore introduced for various cation surfactants detection. (B) Schematic illustration of the production of a fluorescence turn-on PDA sensor for the plasma membrane imaging. This figure was reproduced with permission from ref. (Wang et al., 2016). Copyright 2016, American Chemical Society and (Wang et al., 2020). Copyright 2020, Elsevier B.V.

5. Future perspective

5.1. General challenges of PDA based sensor

Generally, fluorescence-based sensor systems require a low background fluorescence for higher sensitivity. A sensor platform with a low background signal can more sensitively distinguish a signal generated when a target material is present (Jeong et al., 2018; Thomas et al., 2007; Valeur and Leray 2000). From the point of view of the background signal commonly used in the sensor field, the background fluorescence of PDA in the blue state can be considered to be quite low in magnitude. However, when UV is applied to polymerize diacetylene assemblies and if the amount of injected energy is excessive, some diacetylene assemblies may be converted to a red state, causing background fluorescence (Reppy and Pindzola 2007b). Additionally, while various types of receptors, if the topochemical structure between diacetylenes significantly deviates from the conditions for proper polymerization, there is a possibility that polymerization does not occur or a red color state PDA is formed. These factors may cause some errors in the detection of a target material with a PDA fluorescent signal. To solve the modification of PDA due to excessive UV energy irradiation, a DA monomer derivative that can induce relatively strong intermolecular bonds such as hydrogen bonds is used, or it is necessary to perform an optimization process to minimize the formation of the red-state PDA.

Although it is known that the disturbance of the PDA backbone is the main cause of the change in the PDA state, the inaccurate identification of the PDA state change mechanism can also hinder further application (Qian and Stadler 2019). For example, it has not been clearly revealed whether the PDA state change is continuous or non-continuous, that is, whether an intermediate states exist microscopically. It is a great advantage to be able to impart selectivity to a PDA sensor by introducing a receptor suitable for the situation. However, due to the nature of PDA that exhibits fluorescence through interactions, the amount of UV energy to be irradiated and the intensity of the signal can vary depending on the density of receptors and the type of DA monomer. Additionally, since PDA shows a relatively low quantum yield and fluorescence intensity as compared to other nanoparticles or fluorophores, a method to amplify the fluorescent signal of PDA is additionally required.

In addition to the PDA material-based sensor as a chromogenic material or a fluorophore, a platform using electrical signals or other optical methods is being developed (Dubas et al., 2017; Liffmann et al., 2015; Rao et al., 2020). A platform with higher sensitivity than the conventional color change or fluorescence detection method has been developed using the conductivity and optical properties of PDA due to its conjugated bond.

5.2. Various PDA perspectives for sensor applications

PDA sensors are applied to a wider range of applications, including in the role of chemosensors or biosensors, that directly or indirectly detect general target substances (Fang et al., 2020; Wen et al., 2018). For example, PDA nanostructures, such as liposomes or micelles that mimic cell membranes can act as drug delivery carriers for chemotherapy (Yao et al., 2017). The main disadvantages of liposomes composed of general phospholipids are low stability and low delivery efficiency due to drug leakage (Dromi et al., 2007). In contrast, PDA-based liposomes maintain the biocompatibility characteristics of liposomes, and the stability of the membrane is greatly increased due to the conjugated backbone generated through polymerization, which can offset low delivery efficiency to some extent (Bulbake et al., 2017; Qin et al., 2011). In addition, the PDA structure has been used in bioimaging fields because it exhibits red fluorescence *in vivo* or *in vitro* (Tao et al., 2019; Yang et al., 2014a). Functionalized PDA composites become fluorescent when the PDA is exposed to interaction with the target, heat, pH, and others, enabling fluorescence tracking for the movement path (Peng et al., 2017). That is, PDA liposome can simultaneously act as a fluorescent molecule for bioimaging and perform a drug delivery function (Li et al., 2015a; Yan and An 2014).

Additionally, PDA supramolecular structures are also used in fields such as tissue engineering. Through label-free fluorescence of PDA structures stimulated by ligand-receptor interaction, it is possible to check the behavior of cells by introducing functional groups related to cell movement or adhesion (Haridas et al., 2014; Ramakers et al., 2015; Samal et al., 2012). Functionalized PDA, in the form of a film or scaffold, is attracting attention because it not only provides a signal for cell behavior or differentiation, but also enhances the mechanical strength of the scaffold with the unique optical characteristics of the PDA (Biesalski et al., 2006; Das et al., 2019).

PDA, a conductive polymer, has relatively poor electrical conductivity owing to its rigid crystal domain in the bulk phase, but has high electrical conductivity when the nano-sized structure has a one crystal domain through self-assembly (Cho et al., 2011; Marikhin et al., 1997; Nakanishi et al., 1983; Okawa et al., 2012). PDA films or assemblies can be used as a semiconductor electrical conductance because of their high mobility characteristics. In addition, as interest in flexible and stretchable electronics has increased, many studies on microscopic PDA structures with unique optical properties and electrical conductivity have been conducted in the photonics or electronics fields (Girard-Reydet et al., 2016; Yarimaga et al., 2012b). For example, PDA tubes exhibit a unique phenomenon as an optical waveguide and is promising for various sensor applications (Hu et al., 2014; Rao et al., 2020; Zhu et al., 2016).

6. Summary and conclusion

We reviewed the optical behaviors of PDA through the characteristics and structure of various diacetylene monomers and PDA. The diacetylene monomer can be customized to suit the desired structure and has the advantage of being accompanied by color changes observable to the naked eye. Moreover, because PDA exhibits fluorescence “turn-on” characteristics, it is possible to construct a label-free sensor platform and synergize it through collaboration with other fluorophores. We discussed the factors that cause the signal generation of PDA and strategies to improve the sensitivity of advanced sensor platforms. Understanding the optical properties of PDA is important because it improves the capabilities of PDA and enables its application to a wider range of applications. Since the first synthesis of diacetylene and its use in sensor applications, the unique properties of PDA caused by conjugated bonds have been widely used. In addition to color change and fluorescence properties, the unique optical properties of PDA still make PDA attractive. As a type of conjugated polymer with a conjugated bond, PDA has the potential to be applied to fields such as photonics and electronics. To appropriately utilize the potential of PDA, more studies are needed to properly understand the optical properties of PDA and to clarify the mechanism for the optical property change.

Declaration of competing interest

The authors declare that they have no known competing financial interests or personal relationships that could have appeared to influence the work reported in this paper.

Acknowledgement

This paper was supported by The Nano & Material Technology Development Program of the National Research Foundation of Korea (NRF) funded by the Ministry of Science and ICT (grant number: NRF-2017M3A7B4049850).

Appendix A. Supplementary data

Supplementary data to this article can be found online at https://doi.

org/10.1016/j.bios.2021.113120.

References

Aalipour, A., Chuang, H.Y., Murty, S., D'Souza, A.L., Park, S.M., Gulati, G.S., Patel, C.B., Beinat, C., Simonetta, F., Martinic, I., Gowrishankar, G., Robinson, E.R., Aalipour, E., Zhian, Z., Gambhir, S.S., 2019. Nat. Biotechnol. 37 (5), 531-+.

Ahn, D.J., Chae, E.H., Lee, G.S., Shim, H.Y., Chang, T.E., Ahn, K.D., Kim, J.M., 2003. J. Am. Chem. Soc. 125 (30), 8976–8977.

Ahn, D.J., Kim, J.M., 2008. Accounts Chem. Res. 41 (7), 805–816.

Ahn, D.J., Lee, S., Kim, J.-M., 2009. Adv. Funct. Mater. 19 (10), 1483–1496.

Ai, H.W., Hazelwood, K.L., Davidson, M.W., Campbell, R.E., 2008. Nat. Methods 5 (5), 401–403.

Alami, M., Ferri, F., 1996. Tetrahedron Lett. 37 (16), 2763–2766.

Alloisio, M., Zappia, S., Demartini, A., Espinoza, M.I.M., Ottonelli, M., Dellepiane, G., Thea, S., Cavalleri, O., Rolandi, R., 2015. Nano-Structures & Nano-Objects 4, 15–22.

Anker, J.N., Hall, W.P., Lyandres, O., Shah, N.C., Zhao, J., Van Duyne, R.P., 2008. Nat. Mater. 7 (6), 442–453.

Ardona, H.A.M., Tovar, J.D., 2015. Bioconjugate Chem. 26 (12), 2290–2302.

Baek, S., Song, S., Lee, J., Kim, J.-M., 2016. Sensor. Actuator. B Chem. 230, 623–629.

Bandyopadhyay, A., Varghese, B., Sankararaman, S., 2006. J. Org. Chem. 71 (12), 4544–4548.

Bang, J.J., Rupp, K.K., Russell, S.R., Choong, S.W., Claridge, S.A., 2016. J. Am. Chem. Soc. 138 (13), 4448–4457.

Bangham, A., 1989. Cc/Life Sci (13), 14-14.

Batchelder, D.N., Bloor, D., 1982. J Phys C Solid State 15 (13), 3005–3018.

Batchelder, D.N., Evans, S.D., Freeman, T.L., Haussling, L., Ringsdorf, H., Wolf, H., 1994. J. Am. Chem. Soc. 116 (3), 1050–1053.

Batchelder, D.N., Poole, N.J., Bloor, D., 1981. Chem. Phys. Lett. 81 (3), 560–564.

Baughman, R.H., 1972. J. Appl. Phys. 43 (11), 4362-&.

Berman, A., Ahn, D.J., Lio, A., Salmeron, M., Reichert, A., Charych, D., 1995. Science 269 (5223), 515–518.

Biesalski, M.A., Knaebel, A., Tu, R., Tirrell, M., 2006. Biomaterials 27 (8), 1259–1269.

Blaise, P., Breysse, P., Henriroussseau, O., Malrieu, J.P., Maynau, D., 1991. J Mol Struc-Theochem 75, 219–247.

Bloor, D., Worboys, M.R., 1998. J. Mater. Chem. 8 (4), 903–912.

Bulbake, U., Doppalapudi, S., Kommineni, N., Khan, W., 2017. Pharmaceutics 9 (2).

Carpick, R.W., Mayer, T.M., Sasaki, D.Y., Burns, A.R., 2000. Langmuir 16 (10), 4639–4647.

Carpick, R.W., Sasaki, D.Y., Marcus, M.S., Eriksson, M.A., Burns, A.R., 2004. J Phys-Condens Mat 16 (23), R679–R697.

Chae, S., Lee, J.P., Kim, J.M., 2016. Adv. Funct. Mater. 26 (11), 1769–1776.

Chaki, N.K., Vijayamohanan, K., 2002. Biosens. Bioelectron. 17 (1–2), 1–12.

Chanakul, A., Traiphol, N., Traiphol, R., 2013. J. Colloid Interface Sci. 389, 106–114.

Chance, R.R., Baughman, R.H., 1976. J. Chem. Phys. 64 (9), 3889–3890.

Chance, R.R., Baughman, R.H., Muller, H., Eckhardt, C.J., 1977. J. Chem. Phys. 67 (8), 3616–3618.

Chance, R.R., Patel, G.N., Witt, J.D., 1979. J. Chem. Phys. 71 (1), 206–211.

Charoenthai, N., Pattanatornchai, T., Wacharasindhu, S., Sukwattanasinitt, M., Traiphol, R., 2011. J. Colloid Interface Sci. 360 (2), 565–573.

Charron, D.M., Zheng, G., 2018. Nano Today 18, 124–136.

Charych, D., Cheng, Q., Reichert, A., Kuziemko, G., Stroh, M., Nagy, J.O., Spevak, W., Stevens, R.C., 1996. Chem Biol 3 (2), 113–120.

Charych, D.H., Nagy, J.O., Spevak, W., Bednarski, M.D., 1993. Science 261 (5121), 585–588.

Chen, C.F., Chen, J., Wang, T.Y., Liu, M.H., 2016. Acs Appl Mater Inter 8 (44), 30608–30615.

Chen, N.T., Cheng, S.H., Liu, C.P., Souris, J.S., Chen, C.T., Mou, C.Y., Lo, L.W., 2012a. Int. J. Mol. Sci. 13 (12), 16598–16623.

Chen, T.K., He, B., Tao, J.S., He, Y., Deng, H.L., Wang, X.Q., Zheng, Y., 2019. Adv. Drug Deliv. Rev. 143, 177–205.

Chen, X., Tao, J., Zou, G., Su, W., Zhang, Q.J., Liu, S.Y., Wang, P., 2011. Appl Phys a-Mater 102 (3), 565–575.

Chen, X.Q., Zhou, G.D., Peng, X.J., Yoon, J., 2012b. Chem. Soc. Rev. 41 (13), 4610–4630.

Chen, Y.J., Carter, G.M., Koteles, E.S., Elman, B., Georger, J., Tripathy, S., 1984. Journal of the Optical Society of America a-Optics Image Science and Vision 1 (12), 1250-1250.

Chen, Y.J., Carter, G.M., Tripathy, S.K., 1985. Solid State Commun. 54 (1), 19–22.

Cheng, Q., Stevens, R.C., 1997. Adv. Mater. 9 (6), 481 (&).

Cheng, Q., Yamamoto, M., Stevens, R.C., 2000. Langmuir 16 (12), 5333–5342.

Cheng, Y.J., Yang, S.H., Hsu, C.S., 2009. Chem. Rev. 109 (11), 5868–5923.

Cho, E., Kim, H., Choi, Y., Paik, S.R., Jung, S., 2016a. Sci Rep-Uk 6.

Cho, S., Han, G., Kim, K., Sung, M.M., 2011. Angew. Chem. Int. Ed. 50 (12), 2742–2746.

Cho, Y.-S., Ahn, K.H., 2013a. J. Mater. Chem. B 1 (8).

Cho, Y.S., Ahn, K.H., 2013b. J. Mater. Chem. B 1 (8), 1182–1189.

Cho, Y.S., Ma, D.H., Ahn, K.H., 2016b. J. Mater. Chem. C 4 (14), 2871–2876.

Choi, H., Choi, I.S., Lee, G.S., Ahn, D.J., 2011. J. Nanosci. Nanotechnol. 11 (7), 6203–6207.

Chu, B., Xu, R.L., 1991. Accounts Chem. Res. 24 (12), 384–389.

Cui, C., Kim, S., Ahn, D.J., Joo, J., Lee, G.S., Park, D.H., Kim, B.-H., 2018. Synth. Met. 236, 19–23.

Cui, Y., Wei, Q.Q., Park, H.K., Lieber, C.M., 2001. Science 293 (5533), 1289–1292.

Das, E.C., Dhawan, S., Babu, J., Anil Kumar, P., Kumary, T.V., Haridas, V., Komath, M., 2019. J. Periodontal. Res. 54 (5), 468–480.

Dautel, O.J., Robitzer, M., Lere-Porte, J.P., Serein-Spirau, F., Moreau, J.J.E., 2006. J. Am. Chem. Soc. 128 (50), 16213–16223.

de Oliveira, T.V., Soares, N.D.F., Coimbra, J.S.D., de Andrade, N.J., Moura, L.G., Medeiros, E.A.A., de Medeiros, H.S., 2015. Sensor. Actuator. B Chem. 221, 653–658.

de Silva, A.P., Gunaratne, H.Q.N., Gunnlaugsson, T., Huxley, A.J.M., McCoy, C.P., Rademacher, J.T., Rice, T.E., 1997. Chem. Rev. 97 (5), 1515–1566.

Di Benedetto, F., Camposeo, A., Pagliara, S., Mele, E., Persano, L., Stabile, R., Cingolani, R., Pisignano, D., 2008. Nat. Nanotechnol. 3 (10), 614–619.

Dobrosavljevic, V., Stratt, R.M., 1987. Phys. Rev. B 35 (6), 2781–2794.

Dolai, S., Bhunia, S.K., Beglaryan, S.S., Kolusheva, S., Zeiri, L., Jelinek, R., 2017. Acs Appl Mater Inter 9 (3), 2891–2898.

Dromi, S., Frenkel, V., Luk, A., Traughber, B., Angstadt, M., Bur, M., Poff, J., Xie, J.W., Libutti, S.K., Li, K.C.P., Wood, B.J., 2007. Clin. Canc. Res. 13 (9), 2722–2727.

Dubas, A.L., Tameev, A.R., Zvyagina, A.I., Ezhoy, A.A., Ivanov, V.K., Konig, B., Arslanov, V.V., Gribkova, O.L., Kalinina, M.A., 2017. Acs Appl Mater Inter 9 (50), 43838–43845.

Dubertret, B., Calame, M., Libchaber, A.J., 2001. Nat. Biotechnol. 19 (7), 680–681.

Eckhardt, H., Boudreaux, D.S., Chance, R.R., 1986. J. Chem. Phys. 85 (7), 4116–4119.

El-Sayed, I.H., Huang, X.H., El-Sayed, M.A., 2005. Nano Lett. 5 (5), 829–834.

Evans, E., Kwok, R., 1982. Biochemistry 21 (20), 4874–4879.

Exarhos, G.J., Risen, W.M., Baughman, R.H., 1976. J. Am. Chem. Soc. 98 (2), 481–487.

Fang, F., Meng, F.L., Luo, L., 2020. Mater Chem Front 4 (4), 1089–1104.

Feng, H.B., Lu, J., Li, J.H., Tsow, F., Forzani, E., Tao, N.J., 2013. Adv. Mater. 25 (12), 1729–1733.

Ferguson, C.G., James, R.D., Bigman, C.S., Shepard, D.A., Abdiche, Y., Katsamba, P.S., Myszka, D.G., Prestwich, G.D., 2005. Bioconjugate Chem. 16 (6), 1475–1483.

Fischetti, R.F., Filipkowski, M., Garito, A.F., Blasie, J.K., 1988. Phys. Rev. B 37 (9), 4714–4726.

Gaboriaud, F., Golan, R., Volinsky, R., Berman, A., Jelinek, R., 2001. Langmuir 17 (12), 3651–3657.

Geiger, E., Hug, P., Keller, B.A., 2002. Macromol. Chem. Phys. 203 (17), 2422–2431.

Germinario, L.T., Gillette, P.C., 1982. Ultramicroscopy 9 (3), 225–229.

Girard-Reydet, C., Ortuso, R.D., Tsemperouli, M., Sugihara, K., 2016. J. Phys. Chem. B 120 (14), 3511–3515.

Gravel, E., Ogier, J., Arnauld, T., Mackiewicz, N., Duconge, F., Doris, E., 2012. Chem. Eur J. 18 (2), 400–408.

Gregory, J., Exarhos, W.M.R.J., Baughman, Ray H., 1976. J. Am. Chem. Soc. 98 (2), 481–487.

Grimsdale, A.C., Chan, K.L., Martin, R.E., Jokisz, P.G., Holmes, A.B., 2009. Chem. Rev. 109 (3), 897–1091.

Gros, L., Ringsdorf, H., Schupp, H., 1981. Angew. Chem. Int. Ed. 20 (4), 305–325.

Gu, C.C., Geng, Y.Y., Zheng, F., Rotello, V.M., 2020. Analyst 145 (8), 3049–3055.

Gwon, Y.J., Kim, C., Lee, T.S., 2019. Sensor. Actuator. B Chem. 281, 343–349.

Hacia, J.G., Brody, L.C., Chee, M.S., Fodor, S.P.A., Collins, F.S., 1996. Nat. Genet. 14 (4), 441–447.

Haridas, V., Sadanandan, S., Collart-Dutilleul, P.Y., Gronthos, S., Voelcker, N.H., 2014. Biomacromolecules 15 (2), 582–590.

Hattori, T., Kobayashi, T., 1987. Chem. Phys. Lett. 133 (3), 230–234.

He, C.L., Feng, Z.Y., Shan, S.Z., Wang, M.Q., Chen, X., Zou, G., 2020. Nat. Commun. 11 (1).

Heo, J.M., Kim, Y., Han, S., Joung, J.F., Lee, S.H., Han, S., Noh, J., Kim, J., Park, S., Lee, H., Choi, Y.M., Jung, Y.S., Kim, J.M., 2017. Macromolecules 50 (3), 900–913.

Heo, J.M., Son, Y., Han, S., Ro, H.J., Jun, S., Kundapur, U., Noh, J., Kim, J.M., 2019. Macromolecules 52 (11), 4405–4411.

Ho, H.A., Leclerc, M., 2004. J. Am. Chem. Soc. 126 (5), 1384–1387.

Homola, J., 2008. Chem. Rev. 108 (2), 462–493.

Hong, J., Park, D.H., Baek, S., Song, S., Lee, C.W., Kim, J.M., 2015. Acs Appl Mater Inter 7 (15), 8339–8343.

Hood, R.J., Muller, H., Eckhardt, C.J., Chance, R.R., Yee, K.C., 1978. Chem. Phys. Lett. 54 (2), 295–299.

Hu, W.L., Chen, Y.K., Jiang, H., Li, J.G., Zou, G., Zhang, Q.J., Zhang, D.G., Wang, P., Ming, H., 2014. Adv. Mater. 26 (19), 3136–3141.

Huo, J.P., Deng, Q.J., Fan, T., He, G.Z., Hu, X.H., Hong, X.X., Chen, H., Luo, S.H., Wang, Z.Y., Chen, D.C., 2017a. Polym. Chem. 8 (48), 7438–7445.

Huo, J.P., Hu, Z.D., He, G.Z., Hong, X.X., Yang, Z.H., Luo, S.H., Ye, X.F., Li, Y.L., Zhang, Y.B., Zhang, M., Chen, H., Fan, T., Zhang, Y.Y., Xiong, B.Y., Wang, Z.Y., Zhu, Z.B., Chen, D.C., 2017b. Appl. Surf. Sci. 423, 951–956.

Im, H., Shao, H.L., Park, Y.I., Peterson, V.M., Castro, C.M., Weissleder, R., Lee, H., 2014. Nat. Biotechnol. 32 (5), 490-U219.

Inoko, Y., Mitsui, T., 1978. J. Phys. Soc. Jpn. 44 (6), 1918–1924.

Itoh, K., Nishizawa, T., Yamagata, J., Fujii, M., Osaka, N., Kudryashov, I., 2005. J. Phys. Chem. B 109 (1), 264–270.

Jacobs, C.B., Peairs, M.J., Venton, B.J., 2010. Anal. Chim. Acta 662 (2), 105–127.

Jager, E.W.H., Smela, E., Inganas, O., 2000. Science 290 (5496), 1540–1545.

Jang, D., Pramanik, S.K., Das, A., Baek, W., Heo, J.M., Ro, H.J., Jun, S., Park, B.J., Kim, J. M., 2019. Sci Rep-Uk 9.

Jelinek, R., Kolusheva, S., 2001. Biotechnol. Adv. 19 (2), 109–118.

Jelinek, R., Ritenberg, M., 2013. RSC Adv. 3 (44), 21192–21201.

Jeong, Y., Kook, Y.M., Lee, K., Koh, W.G., 2018. Biosens. Bioelectron. 111, 102–116.

Ji, X.F., Yao, Y., Li, J.Y., Yan, X.Z., Huang, F.H., 2013. J. Am. Chem. Soc. 135 (1), 74–77.

Jiang, H., Jelinek, R., 2016. Chempluschem 81 (1), 119–124.

Johnston, D.S., Sanghera, S., Pons, M., Chapman, D., 1980. Biochim. Biophys. Acta 602 (1), 57–69.

Jordan, R.S., Wang, Y., McCurdy, R.D., Yeung, M.T., Marsh, K.L., Khan, S.I., Kaner, R.B., Rubin, Y., 2016. Chem-Us 1 (1), 78–90.

Jose, D.A., Konig, B., 2010. Org. Biomol. Chem. 8 (3), 655–662.

Jung, S.H., Jang, H., Lim, M.C., Kim, J.H., Shin, K.S., Kim, S.M., Kim, H.Y., Kim, Y.R., Jeon, T.J., 2015. Anal. Chem. 87 (4), 2072–2078.
Jung, Y.K., Jung, C., Park, H.G., 2016. Acs Appl Mater Inter 8 (24), 15684–15690.
Jung, Y.K., Kim, T.W., Kim, J., Kim, J.M., Park, H.G., 2008. Adv. Funct. Mater. 18 (5), 701–708.
Jung, Y.K., Kim, T.W., Park, H.G., Soh, H.T., 2010. Adv. Funct. Mater. 20 (18), 3092–3097.
Jung, Y.K., Park, H.G., 2015. Biosens. Bioelectron. 72, 127–132.
Jung, Y.K., Woo, M.A., Soh, H.T., Park, H.G., 2014. Chem Commun 50 (82), 12329–12332.
Kajzar, F., Messier, J., Zyss, J., Ledoux, I., 1983. Optic Commun. 45 (2), 133–137.
Kang, D.H., Jung, H.S., Ahn, N., Lee, J., Seo, S., Suh, K.Y., Kim, J., Kim, K., 2012a. Chem Commun 48 (43), 5313–5315.
Kang, D.H., Jung, H.S., Kim, K., Kim, J., 2017. ACS Appl. Mater. Interfaces 9 (48), 42210–42216.
Kang, D.H., Jung, H.S., Lee, J., Seo, S., Kim, J., Kim, K., Suh, K.Y., 2012b. Langmuir 28 (19), 7551–7556.
Kantha, C., Kim, H., Kim, Y., Heo, J.M., Joung, J.F., Park, S., Kim, J.M., 2018. Dyes Pigments 154, 199–204.
Katrlik, J., Svorc, J., Rosenberg, M., Miertus, S., 1996. Anal. Chim. Acta 331 (3), 225–232.
Kew, S.J., Hall, E.A.H., 2006. Anal. Chem. 78 (7), 2231–2238.
Khanantong, C., Charoenthai, N., Phuangkaew, T., Kielar, F., Traiphol, N., Traiphol, R., 2018. Colloid. Surface. 553, 337–348.
Khanantong, C., Charoenthai, N., Wacharasindhu, S., Sukwattanasinitt, M., Yimkaew, W., Traiphol, N., Traiphol, R., 2020. Colloid. Surface. 603.
Kim, C., Lee, K., 2019. Biomacromolecules 20 (9), 3392–3398.
Kim, H.-M., Kang, Y.-L., Chung, W.-J., Kyeong, S., Jeong, S., Kang, H., Jeong, C., Rho, W.-Y., Kim, D.-H., Jeong, D.H., Lee, Y.-S., Jun, B.-H., 2015a. J. Ind. Eng. Chem. 21, 158–162.
Kim, H.M., Kang, Y.L., Chung, W.J., Kyeong, S., Jeong, S., Kang, H., Jeong, C., Rho, W.Y., Kim, D.H., Jeong, D.H., Lee, Y.S., Jun, B.H., 2015b. J. Ind. Eng. Chem. 21, 158–162.
Kim, J.M., Ji, E.K., Woo, S.M., Lee, H., Ahn, D.J., 2003a. Adv. Mater. 15 (13), 1118–1121.
Kim, J.M., Ji, E.K., Woo, S.M., Lee, H.W., Ahn, D.J., 2003b. Adv. Mater. 15 (13), 1118–+.
Kim, J.M., Lee, J.S., Lee, J.S., Woo, S.Y., Ahn, D.J., 2005a. Macromol. Chem. Phys. 206 (22), 2299–2306.
Kim, J.M., Lee, Y.B., Yang, D.H., Lee, J.S., Lee, G.S., Ahn, D.J., 2005b. J. Am. Chem. Soc. 127 (50), 17580–17581.
Kim, J.P., Kwon, I.K., Sim, S.J., 2011. Biosens. Bioelectron. 26 (12), 4823–4827.
Kim, K., Kim, M.J., Kim, W., Kim, S.Y., Park, S., Park, C.B., 2020a. Nat. Commun. 11 (1).
Kim, K.W., Choi, H., Lee, G.S., Ahn, D.J., Oh, M.K., 2008. Colloids Surf., B 66 (2), 213–217.
Kim, M., Shin, Y.J., Shin, M.J., Shin, J.S., 2017a. J. Appl. Polym. Sci. 134 (26).
Kim, S., Kim, B.H., Hong, Y.K., Cui, C., Choi, J., Park, D.H., Song, S.H., 2020b. Polymers 12 (3).
Kim, S., Lee, S., Ahn, Y., Kim, H.K., Koh, J., Kim, S.D., Kim, B.G., 2017b. J. Mater. Chem. C 5 (33), 8553–8558.
Kim, T.S., Crooks, R.M., Tsen, M., Sun, L., 1995. J. Am. Chem. Soc. 117 (14), 3963–3967.
Kobayashi, T., Yasuda, M., Okada, S., Matsuda, H., Nakanishi, H., 1997. Chem. Phys. Lett. 267 (5–6), 472–480.
Kolusheva, S., Boyer, L., Jelinek, R., 2000a. Nat. Biotechnol. 18 (2), 225–227.
Kolusheva, S., Kafri, R., Katz, M., Jelinek, R., 2001. J. Am. Chem. Soc. 123 (3), 417–422.
Kolusheva, S., Lecht, S., Derazon, Y., Jelinek, R., Lazarovici, P., 2008. Peptides 29 (9), 1620–1625.
Kolusheva, S., Molt, O., Herm, M., Schrader, T., Jelinek, R., 2005. J. Am. Chem. Soc. 127 (28), 10000–10001.
Kolusheva, S., Shahal, T., Jelinek, R., 2000b. J. Am. Chem. Soc. 122 (5), 776–780.
Kolusheva, S., Wachtel, E., Jelinek, R., 2003. JLR (J. Lipid Res.) 44 (1), 65–71.
Kootery, K.P., Jiang, H., Kolusheva, S., Vinod, T.P., Ritenberg, M., Zeiri, L., Volinsky, R., Malferrari, D., Galletti, P., Tagliavini, E., Jelinek, R., 2014. Acs Appl Mater Inter 6 (11), 8613–8620.
Kunitake, T., Okahata, Y., 1977. J. Am. Chem. Soc. 99 (11), 3860–3861.
Kuo, T., Obrien, D.F., 1990. J. Chem. Soc., Chem. Commun. 11, 839–841.
Kuriyama, K., Kikuchi, H., Kajiyama, T., 1996a. Langmuir 12 (26), 6468–6472.
Kuriyama, K., Kikuchi, H., Kajiyama, T., 1996b. Langmuir 12 (9), 2283–2288.
Kuriyama, K., Kikuchi, H., Kajiyama, T., 1998. Langmuir 14 (5), 1130–1138.
Kuroda, K., Swager, T.M., 2003. Macromol. Symp. 201, 127–134.
Kwon, I.K., Kim, J.P., Sim, S.J., 2010. Biosens. Bioelectron. 26 (4), 1548–1553.
Kwon, I.K., Song, M.S., Won, S.H., Choi, S.P., Kim, M., Sim, S.J., 2012. Small 8 (2), 209–213.
Kwon, J.H., Song, J.E., Yoon, B., Kim, J.M., Cho, E.C., 2014. Bull. Kor. Chem. Soc. 35 (6), 1809–1816.
Kyeong, S., Kang, H., Yim, J., Jeon, S.J., Jeong, C.H., Lee, Y.S., Jun, B.H., Kim, J.H., 2013. J. Colloid Interface Sci. 394, 44–48.
Lauher, J.W., Fowler, F.W., Goroff, N.S., 2008. Accounts of Chemical Research 41 (9), 1215–1229.
Lecuiller, R., Berrehar, J., Lapersonne-Meyer, C., Schott, M., Ganiere, J.D., 1999. Chem. Phys. Lett. 314 (3–4), 255–260.
Lee, D.C., Sahoo, S.K., Cholli, A.L., Sandman, D.J., 2002. Macromolecules 35 (11), 4347–4355.
Lee, G.S., Kim, T.Y., Ahn, D.J., 2018a. J. Ind. Eng. Chem. 67, 312–315.
Lee, H.Y., Tiwari, K.R., Raghavan, S.R., 2011. Soft Matter 7 (7), 3273–3276.
Lee, J., Jun, H., Kim, J., 2009a. Adv. Mater. 21 (36), 3674–+.
Lee, J., Jun, H., Kim, J., 2009b. Adv. Mater. 21 (36), 3674–3677.
Lee, J., Kim, H.J., Kim, J., 2008. J. Am. Chem. Soc. 130 (15), 5010–+.
Lee, J., Kim, J., 2012. Chem. Mater. 24 (14), 2817–2822.
Lee, J., Pyo, M., Lee, S.H., Kim, J., Ra, M., Kim, W.Y., Park, B.J., Lee, C.W., Kim, J.M., 2014a. Nat. Commun. 5.
Lee, J., Seo, S., Kim, J., 2018b. Acs Appl Mater Inter 10 (4), 3164–3169.
Lee, J.U., Jeong, J.H., Lee, D.S., Sim, S.J., 2014b. Biosens. Bioelectron. 61, 314–320.
Lee, S., Cheng, H., Chi, M., Xu, Q., Chen, X., Eom, C.Y., James, T.D., Park, S., Yoon, J., 2016a. Biosens. Bioelectron. 77, 1016–1019.
Lee, S., Kim, J.Y., Chen, X.Q., Yoon, J., 2016b. Chem Commun 52 (59), 9178–9196.
Lee, S., Lee, J., Lee, D.W., Kim, J.M., Lee, H., 2016c. Chem Commun (Camb) 52 (5), 926–929.
Lee, S., Lee, J., Lee, M., Cho, Y.K., Baek, J., Kim, J., Park, S., Kim, M.H., Chang, R., Yoon, J., 2014c. Adv. Funct. Mater. 24 (24), 3699–3705.
Lee, S.B., Koepsel, R., Stolz, D.B., Warriner, H.E., Russell, A.J., 2004. J. Am. Chem. Soc. 126 (41), 13400–13405.
Li, L.L., An, X.Q., Yan, X.J., 2015a. Colloids Surf., B 134, 235–239.
Li, M., Song, M.Y., Wu, G.T., Tang, Z.Y., Sun, Y.F., He, Y.B., Li, J.H., Li, L., Gu, H.S., Liu, X., Ma, C., Peng, Z.F., Ai, Z.Q., Lewis, D.J., 2017a. Small 13 (21).
Li, S., Zhang, L., Jiang, J., Meng, Y., Liu, M., 2017b. ACS Appl. Mater. Interfaces 9 (42), 37386–37394.
Li, X., Matthews, S., Kohli, P., 2008. J. Phys. Chem. B 112 (42), 13263–13272.
Li, Y., Wang, L.H., Wen, Y.N., Ding, B., Sun, G., Ke, T., Chen, J.Y., Yu, J.Y., 2015b. J. Mater. Chem. 3 (18), 9722–9730.
Li, Y., Wang, L.H., Yin, X., Ding, B., Sun, G., Ke, T., Chen, J.Y., Yu, J.Y., 2014. J. Mater. Chem. 2 (43), 18304–18312.
Liang, J.J., Huang, L., Li, N., Huang, Y., Wu, Y.P., Fang, S.L., Oh, J., Kozlov, M., Ma, Y.F., Li, F.F., Baughman, R., Chen, Y.S., 2012. ACS Nano 6 (12), 11097-11097.
Lichtman, J.W., Conchello, J.A., 2005. Nat. Methods 2 (12), 910–919.
Lieser, G., Tieke, B., Wegner, G., 1980. Thin Solid Films 68 (1), 77–90.
Liffmann, R., Homberger, M., Mennicken, M., Karthauser, S., Simon, U., 2015. RSC Adv. 5 (125), 102981–102992.
Lifshitz, Y., Golan, Y., Konovalov, O., Berman, A., 2009. Langmuir 25 (8), 4469–4477.
Lifshitz, Y., Upcher, A., Kovalev, A., Wainstein, D., Rashkovsky, A., Zeiri, L., Golan, Y., Berman, A., 2011. Soft Matter 7 (19), 9069–9077.
Lim, C.Z.J., Zhang, Y., Chen, Y., Zhao, H.T., Stephenson, M.C., Ho, N.R.Y., Chen, Y., Chung, J., Reilhac, A., Loh, T.P., Chen, G.L.H., Shao, H.L., 2019. Nat. Commun. 10.
Lim, M.C., Shin, Y.J., Jeon, T.J., Kim, H.Y., Kim, Y.R., 2011. Anal. Bioanal. Chem. 400 (3), 777–785.
Lin, K.C., Weis, R.M., Mcconnell, H.M., 1982. Nature 296 (5853), 164–165.
Lio, A., Reichert, A., Ahn, D.J., Nagy, J.O., Salmeron, M., Charych, D.H., 1997. Langmuir 13 (24), 6524–6532.
Lio, A., Reichert, A., Nagy, J.O., Salmeron, M., Charych, D.H., 1996. J Vac Sci Technol B 14 (2), 1481–1485.
Lochner, K., Reimer, B., Bassler, H., 1976. Chem. Phys. Lett. 41 (2), 388–390.
Lu, Y.F., Yang, Y., Sellinger, A., Lu, M.C., Huang, J.M., Fan, H.Y., Haddad, R., Lopez, G., Burns, A.R., Sasaki, D.Y., Shelnutt, J., Brinker, C.J., 2001. Nature 410 (6831), 913–917.
Ma, G.Y., Cheng, Q., 2005. Langmuir 21 (14), 6123–6126.
Ma, G.Y., Muller, A.M., Bardeen, C.J., Cheng, Q., 2006. Adv. Mater. 18 (1), 55–60.
Ma, Z.F., Li, J.R., Liu, M.H., Cao, J., Zou, Z.Y., Tu, J., Jiang, L., 1998. J. Am. Chem. Soc. 120 (48), 12678–12679.
Mapazi, O., Matabola, K.P., Moutloali, R.M., Ngila, C.J., 2018. Polymer 149, 106–116.
Marikhin, V.A., Guk, E.G., Myasnikova, L.P., 1997. Phys. Solid State 39 (4), 686–689.
McQuade, D.T., Pullen, A.E., Swager, T.M., 2000. Chem. Rev. 100 (7), 2537–2574.
Meng, Y., Jiang, J., Liu, M.H., 2017. Nanoscale 9 (21), 7199–7206.
Menzel, H., Horstmann, S., Mowery, M.D., Cai, M., Evans, C.E., 2000. Polymer 41 (22), 8113–8119.
Menzel, H., Mowery, M.D., Cai, M., Evans, C.E., 1998. J. Phys. Chem. B 102 (47), 9550–9556.
Menzel, H., Mowery, M.D., Cai, M., Evans, C.E., 1999. Macromol. Symp. 142, 23–31.
Mino, N., Tamura, H., Ogawa, K., 1991. Langmuir 7 (10), 2336–2341.
Morgan, J., Rumbles, G., Crystall, B., Smith, T.A., Bloor, D., 1992. Chem. Phys. Lett. 196 (5), 455–461.
Mowery, M.D., Menzel, H., Cai, M., Evans, C.E., 1998. Langmuir 14 (19), 5594–5602.
Muller, H., Eckhardt, C.J., 1978. Mol. Cryst. Liq. Cryst. 45 (3–4), 313-&.
Nakanishi, H., Mizutani, F., Kato, M., Hasumi, K., 1983. J Polym Sci Pol Lett 21 (12), 983–987.
Nava, A.D., Thakur, M., Tonelli, A.E., 1990. Macromolecules 23 (12), 3055–3063.
Nguyen-Ngoc, H., Tran-Minh, C., 2007. Anal. Chim. Acta 583 (1), 161–165.
Nguyen, L.H., Naficy, S., McConchie, R., Dehghani, F., Chandrawati, R., 2019. J. Mater. Chem. C 7 (7), 1919–1926.
Nishihara, Y., Ikegashira, K., Mori, A., Hiyama, T., 1998. Tetrahedron Lett. 39 (23), 4075–4078.
Nopwinyuwong, A., Kitaoka, T., Boonsupthip, W., Pechyen, C., Suppakul, P., 2014. Appl. Surf. Sci. 314, 426–432.
Oh, S., Uh, K., Jeon, S., Kim, J.M., 2016. Macromolecules 49 (16), 5841–5848.
Oikawa, H., Korenaga, T., Okada, S., Nakanishi, H., 1999. Polymer 40 (22), 5993–6001.
Okada, S., Peng, S., Spevak, W., Charych, D., 1998. Accounts Chem. Res. 31 (5), 229–239.
Okaniwa, M., Oaki, Y., Kaneko, S., Ishida, K., Maki, H., Imai, H., 2015. Chem. Mater. 27 (7), 2627–2632.
Okawa, Y., Akai-Kasaya, M., Kuwahara, Y., Mandal, S.K., Aono, M., 2012. Nanoscale 4 (10), 3013–3028.
Olmsted, J., Strand, M., 1983. J Phys Chem-Us 87 (24), 4790–4792.
Ostroverkhova, O., 2016. Chem. Rev. 116 (22), 13279–13412.
Pakhomov, S., Hammer, R.P., Mishra, B.K., Thomas, B.N., 2003a. Proc. Natl. Acad. Sci. U. S. A. 100 (6), 3040–3042.

Pakhomov, S., Hammer, R.P., Mishra, B.K., Thomas, B.N., 2003b. P Natl Acad Sci USA 100 (6), 3040–3042.
Pan, J.J., Charych, D., 1997. Langmuir 13 (6), 1365–1367.
Park, C.H., Kim, J.P., Lee, S.W., Jeon, N.L., Yoo, P.J., Sim, S.J., 2009. Adv. Funct. Mater. 19 (23), 3703–3710.
Park, D.H., Hong, J., Park, I.S., Lee, C.W., Kim, J.M., 2014. Adv. Funct. Mater. 24 (33), 5186–5193.
Park, D.H., Jeong, W., Seo, M., Park, B.J., Kim, J.M., 2016a. Adv. Funct. Mater. 26 (4), 498–506.
Park, I.S., Park, H.J., Jeong, W., Nam, J., Kang, Y., Shin, K., Chung, H., Kim, J.M., 2016b. Macromolecules 49 (4), 1270–1278.
Park, J., Ku, S.K., Seo, D., Hur, K., Jeon, H., Shvartsman, D., Seok, H.K., Mooney, D.J., Lee, K., 2016c. Chem Commun (Camb) 52 (68), 10346–10349.
Park, M.K., Kim, K.W., Ahn, D.J., Oh, M.K., 2012. Biosens. Bioelectron. 35 (1), 44–49.
Park, S., Lee, G.S., Cui, C.Z., Ahn, D.J., 2016d. Macromol. Res. 24 (4), 380–384.
Peek, B.M., Callahan, J.H., Namboodiri, K., Singh, A., Gaber, B.P., 1994. Macromolecules 27 (1), 292–297.
Peng, H., Sun, X., Cai, F., Chen, X., Zhu, Y., Liao, G., Chen, D., Li, Q., Lu, Y., Zhu, Y., Jia, Q., 2009. Nat. Nanotechnol. 4 (11), 738–741.
Peng, S., Pan, Y.C., Wang, Y.L., Xu, Z., Chen, C., Ding, D., Wang, Y.J., Guo, D.S., 2017. Adv. Sci. 4 (11).
Peter, J., Hutter, W., Stollnberger, W., Hampel, W., 1996. Biosens. Bioelectron. 11 (12), 1215–1219.
Pevzner, A., Kolusheva, S., Orynbayeva, Z., Jelinek, R., 2008. Adv. Funct. Mater. 18 (2), 242–247.
Phonchai, N., Khanantong, C., Kielar, F., Traiphol, R., Traiphol, N., 2019. Acs Appl Nano Mater 2 (7), 4489–4498.
Pindzola, B.A., Nguyen, A.T., Reppy, M.A., 2006. Chem Commun (8), 906–908.
Potai, R., Faisadcha, K., Traiphol, R., Traiphol, N., 2018. Colloid. Surface. 555, 27–36.
Qian, X.M., Stadler, B., 2019. Chem. Mater. 31 (4), 1196–1222.
Qin, G.T., Li, Z., Xia, R.M., Li, F., O'Neill, B.E., Goodwin, J.T., Khant, H.A., Chiu, W., Li, K.C., 2011. Nanotechnology 22 (15).
Rajesh, Ahuja, T., Kumar, D., 2009. Sensor. Actuator. B Chem. 136 (1), 275–286.
Ramakers, B.E.I., Bode, S.A., Killaars, A.R., van Hest, J.C.M., Lowik, D.W.P.M., 2015. J. Mater. Chem. B 3 (15), 2954–2961.
Rangin, M., Basu, A., 2004. J. Am. Chem. Soc. 126 (16), 5038–5039.
Rao, V.K., Shauloff, N., Sui, X., Wagner, H.D., Jelinek, R., 2020. J. Mater. Chem. C 8 (18), 6034–6041.
Reichert, A., Nagy, J.O., Spevak, W., Charych, D., 1995. J. Am. Chem. Soc. 117 (2), 829–830.
Reppy, M.A., Pindzola, B.A., 2007a. Chem Commun (42), 4317–4338.
Reppy, M.A., Pindzola, B.A., 2007b. Chem Commun (Camb) (42), 4317–4338.
Reshetilov, A.N., Iliasov, P.V., Donova, M.V., Dovbnya, D.V., Boronin, A.M., Leathers, T. D., Greene, R.V., 1997. Biosens. Bioelectron. 12 (3), 241–247.
Rhodes, D.G., Xu, Z.C., Bittman, R., 1992. Biochim. Biophys. Acta 1128 (1), 93–104.
Ringsdorf, H., Schlarb, B., Venzmer, J., 1988. Angew. Chem. Int. Ed. 27 (1), 113–158.
Samal, S.K., Dash, M., Van Vlierberghe, S., Kaplan, D.L., Chiellini, E., van Blitterswijk, C., Moroni, L., Dubruel, P., 2012. Chem. Soc. Rev. 41 (21), 7147–7194.
Sandman, D.J., Chen, Y.J., 1989. Polymer 30 (6), 1027–1031.
Schnur, J.M., Ratna, B.R., Selinger, J.V., Singh, A., Jyothi, G., Easwaran, K.R., 1994a. Science 264 (5161), 945–947.
Schnur, J.M., Ratna, B.R., Selinger, J.V., Singh, A., Jyothi, G., Easwaran, K.R.K., 1994b. Science 264 (5161), 945–947.
Seo, D., Kim, J., 2010. Adv. Funct. Mater. 20 (9), 1397–1403.
Seo, S., Lee, J., Choi, E.J., Kim, E.J., Song, J.Y., Kim, J., 2013. Macromol. Rapid Commun. 34 (9), 743–748.
Seo, S., Lee, J., Kwon, M.S., Seo, D., Kim, J., 2015. Acs Appl Mater Inter 7 (36), 20342–20348.
Seto, K., Hosoi, Y., Furukawa, Y., 2007. Chem. Phys. Lett. 444 (4–6), 328–332.
Sheth, S.R., Leckband, D.E., 1997. Langmuir 13 (21), 5652–5662.
Shimogaki, T., Matsumoto, A., 2011. Macromolecules 44 (9), 3323–3327.
Shin, M.J., Kim, J.D., 2016. Langmuir 32 (3), 882–888.
Shin, M.J., Kim, Y.J., Kim, J.D., 2015. Soft Matter 11 (34), 6903–6904.
Shin, Y.J., Shin, M.J., Shin, J.S., 2017. Colloid. Surface. 520, 459–466.
Singh, Y., Jayaraman, N., 2016. Macromol. Chem. Phys. 217 (8), 940–950.
Smela, E., 2003. Adv. Mater. 15 (6), 481–494.
Song, J., Cisar, J.S., Bertozzi, C.R., 2004. J. Am. Chem. Soc. 126 (27), 8459–8465.
Spevak, W., Nagy, J.O., Charych, D.H., 1995. Adv. Mater. 7 (1), 85–89.
Su, Y.L., Li, J.R., Jiang, L., 2004. Colloids Surf. B Biointerfaces 38 (1–2), 29–33.
Sullivan, S.P., Schnieders, A., Mbugua, S.K., Beebe Jr., T.P., 2005. Langmuir 21 (4), 1322–1327.
Sun, X., Chen, T., Huang, S., Li, L., Peng, H., 2010. Chem. Soc. Rev. 39 (11), 4244–4257.
Tachibana, H., Yamanaka, Y., Sakai, H., Abe, M., Matsumoto, M., 1999. Macromolecules 32 (25), 8306–8309.
Tanaka, H., Gomez, M.A., Tonelli, A.E., Thakur, M., 1989. Macromolecules 22 (3), 1208–1215.
Tao, J., Xu, X., Wang, S., Kang, T.Y., Guo, C.Z., Liu, X., Cheng, H., Liu, Y., Jiang, X., Mao, J., Gou, M.L., 2019. ACS Macro Lett. 8 (5), 563–568.
Thomas, S.W., Joly, G.D., Swager, T.M., 2007. Chem. Rev. 107 (4), 1339–1386.
Tomioka, Y., Tanaka, N., Imazeki, S., 1989. J. Chem. Phys. 91 (9), 5694–5700.
Valeur, B., Leray, I., 2000. Coord. Chem. Rev. 205, 3–40.
Vizgert, R.V., Korostylev, A.P., Krutko, I.N., Zenkova, S.Y., Yenya, V.I., 1989. Vysokomol. Soedin. B 31 (3), 185–187.
Volinsky, R., Kliger, M., Sheynis, T., Kolusheva, S., Jelinek, R., 2007. Biosens. Bioelectron. 22 (12), 3247–3251.
Vollmer, F., Arnold, S., 2008. Nat. Methods 5 (7), 591–596.
Wacharasindhu, S., Montha, S., Boonyiseng, J., Potisatityuenyong, A., Phollookin, C., Tumcharern, G., Sukwattanasinitt, M., 2010. Macromolecules 43 (2), 716–724.
Wang, C., Ma, Z., 2005. Anal. Bioanal. Chem. 382 (7), 1708–1710.
Wang, D.E., Gao, X.H., You, S.Q., Chen, M., Ren, L., Sun, W.J., Yang, H., Xu, H.Y., 2020. Sensor. Actuator. B Chem. 309.
Wang, D.E., Wang, Y.L., Tian, C., Zhang, L.L., Han, X., Tu, Q., Yuan, M.S., Chen, S., Wang, J.Y., 2015. J. Mater. Chem. 3 (43), 21690–21698.
Wang, D.E., Yan, J., Jiang, J., Liu, X., Tian, C., Xu, J., Yuan, M.S., Han, X., Wang, J., 2018a. Nanoscale 10 (9), 4570–4578.
Wang, D.E., Zhao, L., Yuan, M.S., Chen, S.W., Li, T., Wang, J., 2016. ACS Appl. Mater. Interfaces 8 (41), 28231–28240.
Wang, G.J., Hollingsworth, R.I., 1999. Langmuir 15 (9), 3062–3069.
Wang, G.J., Hollingsworth, R.I., 2000. Adv. Mater. 12 (12), 871–874.
Wang, H., Han, S.H., Hu, Y.F., Qi, Z.M., Hu, C.S., 2017a. Colloid. Surface. 517, 84–95.
Wang, M.Q., Yu, Y., Liu, F.N., Ren, L., Zhang, Q.J., Zou, G., 2018b. Talanta 188, 27–34.
Wang, S., Zhang, L.Q., Wan, S., Cansiz, S., Cui, C., Liu, Y., Cai, R., Hong, C.Y., Teng, I.T., Shi, M.L., Wu, Y., Dong, Y.Y., Tan, W.H., 2017b. ACS Nano 11 (4), 3943–3949.
Wang, S.P., Ramirez, J., Chen, Y.S., Wang, P.G., Leblanc, R.M., 1999. Langmuir 15 (17), 5623–5629.
Wang, X.N., Sun, X.L., Hu, P.A., Zhang, J., Wang, L.F., Feng, W., Lei, S.B., Yang, B., Cao, W.W., 2013. Adv. Funct. Mater. 23 (48), 6044–6050.
Wegner, G., 1969. Z Naturforsch Pt B B 24 (7), 824 (&).
Wei, M.L., Liu, J.J., Xia, Y.Y., Feng, F., Liu, W.Y., Zheng, F., 2015. RSC Adv. 5 (81), 66420–66425.
Wen, J.T., Roper, J.M., Tsutsui, H., 2018. Ind. Eng. Chem. Res. 57 (28), 9037–9053.
Weston, M., Kuchel, R.P., Ciftci, M., Boyer, C., Chandrawati, R., 2020. J. Colloid Interface Sci. 572, 31–38.
Won, S.H., Sim, S.J., 2012. Analyst 137 (5), 1241–1246.
Wu, J., Zawistowski, A., Ehrmann, M., Yi, T., Schmuck, C., 2011a. J. Am. Chem. Soc. 133 (25), 9720–9723.
Wu, J.C., Zawistowski, A., Ehrmann, M., Yi, T., Schmuck, C., 2011b. J. Am. Chem. Soc. 133 (25), 9720–9723.
Wu, S., Pan, L.B., Huang, Y.J., Yang, N., Zhang, Q.J., 2018. Soft Matter 14 (33), 6929–6937.
Wu, W., Zhang, J., Zheng, M., Zhong, Y., Yang, J., Zhao, Y., Wu, W., Ye, W., Wen, J., Wang, Q., Lu, J., 2012. PloS One 7 (11), e48999.
Xia, H., Chen, Y., Yang, G., Zou, G., Zhang, Q., Zhang, D., Wang, P., Ming, H., 2014. ACS Appl. Mater. Interfaces 6 (17), 15466–15471.
Xu, Q., Lee, S., Cho, Y., Kim, M.H., Bouffard, J., Yoon, J., 2013a. J. Am. Chem. Soc. 135 (47), 17751–17754.
Xu, Y., Fu, S., Liu, F., Yu, H., Gao, J., 2018. Soft Matter 14 (39), 8044–8050.
Xu, Y., Jiang, H., Zhang, Q., Wang, F., Zou, G., 2014a. Chem Commun (Camb) 50 (3), 365–367.
Xu, Y.Y., Li, J.G., Hu, W.L., Zou, G., Zhang, Q.J., 2013b. J. Colloid Interface Sci. 400, 116–122.
Xu, Y.Y., Yang, G., Xia, H.Y., Zou, G., Zhang, Q.J., Gao, J.G., 2014b. Nat. Commun. 5.
Yager, P., Schoen, P.E., 1984. Mol. Cryst. Liq. Cryst. 106 (3–4), 371–381.
Yager, P., Schoen, P.E., Davies, C., Price, R., Singh, A., 1985. Biophys. J. 48 (6), 899–906.
Yager, P., Sheridan, J.P., Peticolas, W.L., 1982. Biochim. Biophys. Acta 693 (2), 485–491.
Yan, X., An, X., 2014. RSC Adv. 4 (36), 18604–18607.
Yang, D.L., Zou, R.F., Zhu, Y., Liu, B., Yao, D.F., Jiang, J.J., Wu, J.C., Tian, H., 2014a. Nanoscale 6 (24), 14772–14783.
Yang, G., Hu, W.L., Xia, H.Y., Zou, G., Zhanga, Q.J., 2014b. J. Mater. Chem. 2 (37), 15560–15565.
Yao, D.F., Li, S., Zhu, X.M., Wu, J.C., Tian, H., 2017. Chem Commun 53 (7), 1233–1236.
Yapor, J.P., Alharby, A., Gentry-Weeks, C., Reynolds, M.M., Alam, A.K.M.M., Li, Y.V., 2017. ACS Omega 2 (10), 7334–7342.
Yarimaga, O., Jaworski, J., Yoon, B., Kim, J.M., 2012a. Chem Commun (Camb) 48 (19), 2469–2485.
Yarimaga, O., Jaworski, J., Yoon, B., Kim, J.M., 2012b. Chem Commun 48 (19), 2469–2485.
Yasuda, A., Yoshizawa, M., Kobayashi, T., 1993. Chem. Phys. Lett. 209 (3), 281–286.
Yokoyama, T., Masuhara, A., Onodera, T., Kasai, H., Oikawa, H., 2009. Synth. Met. 159 (9–10), 897–899.
Yoon, B., Ham, D.Y., Yarimaga, O., An, H., Lee, C.W., Kim, J.M., 2011. Adv Mater 23 (46), 5492–5497.
Yoon, B., Lee, J., Park, I.S., Jeon, S., Lee, J., Kim, J.M., 2013. J. Mater. Chem. C 1 (13), 2388–2403.
Yoon, B., Lee, S., Kim, J.M., 2009a. Chem. Soc. Rev. 38 (7), 1958–1968.
Yoon, J., Jung, Y.S., Kim, J.M., 2009b. Adv. Funct. Mater. 19 (2), 209–214.
Zhang, P., Zhang, C., Shu, B., 2016a. Sensor. Actuator. B Chem. 236, 27–34.
Zhang, P., Zhang, C.S., Shu, B.W., 2016b. Sensor. Actuator. B Chem. 236, 27–34.
Zhang, X., Yin, J., Yoon, J., 2014. Chem. Rev. 114 (9), 4918–4959.
Zhang, Y., Bromberg, L., Lin, Z., Brown, P., Van Voorhis, T., Hatton, T.A., 2018a. J. Colloid Interface Sci. 528, 27–35.
Zhang, Y.S., Khademhosseini, A., 2017. Science 356 (6337).
Zhang, Z.J., Wei, T.W., Chen, Y.H., Chen, T.T., Chi, B., Wang, F., Chen, X.Q., 2018b. Sensor. Actuator. B Chem. 255, 2211–2217.
Zhu, Y., Qiu, D., Yang, G., Wang, M.Q., Zhang, Q.J., Wang, P., Ming, H., Zhang, D.G., Yu, Y., Zou, G., Badugu, R., Lakowicz, J.R., 2016. Biosens. Bioelectron. 85, 198–204.